

Learning the Transformer Kernel

Sankalan Pal Chowdhury
Department of Computer Science
ETH Zürich

spalchowd@inf.ethz.ch

Adamos Solomou
Department of Computer Science
ETH Zürich

solomou.adamos@gmail.com

Avinava Dubey
Google Research
Mountain View, CA

avinavadubey@google.com

Mrinmaya Sachan
Department of Computer Science
ETH Zürich

mrinmaya.sachan@inf.ethz.ch

Reviewed on OpenReview: <https://openreview.net/forum?id=tLIBAEYjcv>

Abstract

In this work we introduce KL-TRANSFORMER, a generic, scalable, data driven framework for learning the kernel function in Transformers. Our framework approximates the Transformer kernel as a dot product between spectral feature maps and learns the kernel by learning the spectral distribution. This not only helps in learning a generic kernel end-to-end, but also reduces the time and space complexity of Transformers from quadratic to linear. We show that KL-TRANSFORMERS achieve performance comparable to existing efficient Transformer architectures, both in terms of accuracy and computational efficiency. Our study also demonstrates that the choice of the kernel has a substantial impact on performance, and kernel learning variants are competitive alternatives to fixed kernel Transformers, both in long as well as short sequence tasks. ¹

1 Introduction

Transformer models (Vaswani et al., 2017) have demonstrated impressive results on a variety of tasks dealing with language understanding (Devlin et al., 2019; Radford et al., 2018; Raffel et al., 2020; Brown et al., 2020), image processing (Parmar et al., 2018; Carion et al., 2020; Lu et al., 2019), as well as biomedical informatics (Rives et al., 2020; Ingraham et al., 2019; Madani et al., 2020). Albeit powerful, due to the global receptive field of self-attention, the time and memory complexity of Softmax Transformer models scale quadratically with respect to the sequence length. As a result, the application of Transformers to domains with long contexts is rather limited. This limitation has spawned several efficient Transformer designs (Liu et al., 2018; Parmar et al., 2018; Child et al., 2019; Zaheer et al., 2020; Beltagy et al., 2020; Roy et al., 2020; Tay et al., 2020a; Kitaev et al., 2020). Kernelization offers one such design. The use of kernel feature maps allows to reformulate the computation of attention in a way that avoids the explicit computation of the full attention matrix which is the key bottleneck for Softmax Transformer. This also opens up new directions for more generic attention mechanisms.

Tsai et al. (2019) first proposed a kernel-based formulation of the attention mechanism. However, the time and memory complexity of their approach remains quadratic with respect to the sequence length. To address this limitation, Katharopoulos et al. (2020) expressed self-attention as the inner product of kernel feature maps and made use of the

¹Our code and models are available at <https://github.com/cs1160701/OnLearningTheKernel>

associative property to reduce the complexity from quadratic to linear. For their experiments, they used the arbitrarily chosen LinearElu feature map $f(x) = \max(x+1, e^x)$. Performer (Choromanski et al., 2021b) replaces this with feature maps that can directly approximate the softmax kernel, thereby allowing the use of pre-trained Softmax Transformer weights in a linear time model. Concurrently with them, Peng et al. (2021) proposed a linear space and time method that added causal and recency based features to random Fourier methods. More recently, Schlag et al. (2021b) showed the formal equivalence of linearized self-attention mechanisms and fast weight programmers. While the aforementioned approaches provide a significant reduction in computational and memory requirements, this often comes at the cost of performance, as can be seen from Fig. 1. In this work, we posit that this is partly due to the fact that the similarity functions/kernels, including scaled-dot-product, were hand picked and not learnt from data. Thus, we explore whether kernel learning can help to bridge this gap in performance while retaining the scalability of efficient Transformers.

Although, to the best of our knowledge, kernel learning has never been explored within the framework of Transformers, kernel learning methods have been an ubiquitous tool in machine learning. The most notable among them is Random Kitchen Sinks (RKS; Rahimi & Recht, 2007), a data-independent framework for approximating shift-invariant kernels using an explicit feature map. In RKS, the kernel is approximated by $\kappa(x, y) \approx \langle \phi(x), \phi(y) \rangle$, where the explicit feature map $\phi : \mathbb{R}^d \rightarrow \mathbb{R}^s$ is obtained by sampling from a spectral distribution defined by the inverse Fourier transform of the kernel function κ . Wilson & Adams (2013) modeled the spectral density as a mixture of Gaussians, A la Carte (Yang et al., 2015) proposed an optimization based framework for learning the spectral distribution, BaNK (Oliva et al., 2016) modeled the spectral distribution using an infinite mixture of Gaussians, while Fang et al. (2020) implicitly modeled it using deep generative models. We build on these advances and incorporate them into the Transformer framework.

Contributions: In this work, we propose KL-TRANSFORMER, a scalable data driven framework for learning the kernel of Transformers and investigate whether a fully learnable kernel can help to improve the performance of linear, fixed kernel Transformers. Thus, we introduce Transformers with learnable similarity functions, which happen to retain the linear complexity in terms of the sequence length. We motivate our learning method using RKS and learn the kernel by learning the corresponding spectral distribution. In §2.1 we first propose to learn a generic Transformer kernel by explicitly approximating the spectral distribution using a Mixture of Gaussians (GMM) and propose modifications to scale it further. In an attempt to further explore the trade off between computational complexity and accuracy we also propose to model the spectral frequency distribution of Transformer kernels implicitly by using deep generative models (Goodfellow et al., 2014). Finally, we also propose a novel method to learn the spectral distribution of positive random feature (PRF) maps, which provides a better approximation of the softmax kernel (Choromanski et al., 2021b).

We analyse the expressivity and precision of our proposed models (§2.2) and show that the proposed GMM with positional encodings is Turing-complete (Pérez et al., 2019) with controllable variance. We experimentally evaluate our models on *LRA* (tasks with long context), *GLUE* (tasks with short context) and a synthetic dataset with controllable sparsity, and analyze the performance of our models (§3, §2.2). In our experiments, we find that learnt kernels improve performance in long-context tasks, while staying competitive to the Softmax Transformer of the same size in short-context tasks.

We also find that our models learn parameters that reduce the variance in their predictions, and can handle sparsity quite well. We also benchmark the computational efficiency of KL-TRANSFORMERS and find that each of our proposed KL-TRANSFORMERS scales linearly with respect to the sequence length. We conclude with a short comparison between Random Kitchen Sinks (RKS, Rahimi & Recht (2007)) and Positive Random Features Choromanski et al. (2021b) in terms of their performance and provide recommendations on which approach should be chosen under which circumstances.

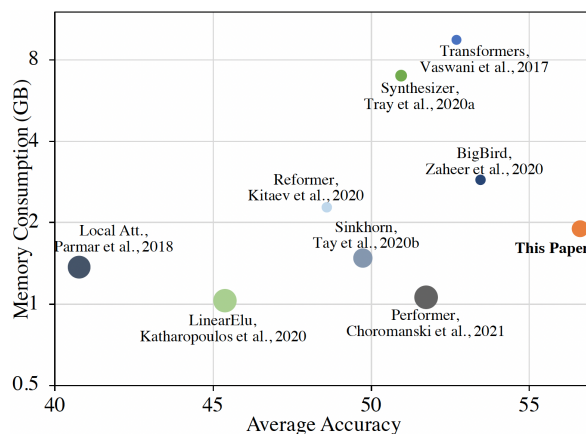


Figure 1: Peak memory (y-axis), average performance (x-axis) and speed (denoted by area of circle) for various efficient Transformer models (i.e. bigger circles in the bottom right corner are better) across three long sequence tasks (> 1024 tokens) introduced in *LRA* (Tay et al., 2021b). All values except for “This Paper” are taken from Tay et al. (2021b).

2 Kernel Learning in Transformers

We begin with the generalized formulation of self-attention proposed by Tsai et al. (2019). Given a non-negative kernel function $\kappa(\cdot, \cdot) : \mathbb{R}^{d_k} \times \mathbb{R}^{d_k} \rightarrow \mathbb{R}_+$, the output of the generalized self-attention mechanism at index i operating on an input sequence $X = (x_1, \dots, x_L) \in \mathbb{R}^{L \times d}$ is defined as

$$\text{ATTN}(X)_i = \sum_{j=1}^L \frac{\kappa(q_i, k_j)}{\sum_{j'=1}^L \kappa(q_i, k_{j'})} v_j. \quad (1)$$

where $k_i = x_i W^K$, $q_i = x_i W^Q$, $v_i = x_i W^V$ are linear transformations of the input sequence into keys, queries and values of dimension $d_q = d_k$ and d_v respectively and $W^K \in \mathbb{R}^{d \times d_k}$, $W^Q \in \mathbb{R}^{d \times d_q}$, $W^V \in \mathbb{R}^{d \times d_v}$. While the formulation in Eq. (1) is more generic and defines a larger space of attention functions, it suffers from a quadratic time and memory complexity. To reduce the quadratic time and memory, we briefly review the method of random Fourier features for the approximation of kernels (Rahimi & Recht, 2007). The details of the method will help motivate and explain our models.

Random Fourier Features for Kernels: At the heart of this method lies the theorem of Bochner (Rudin, 1990) which states that a continuous shift invariant kernel $\kappa(q, k) = \tilde{\kappa}(q - k)$ over arbitrary variables q and k is a positive definite function if and only if $\tilde{\kappa}(\delta)$ is the Fourier transform of a non-negative measure $\rho(\omega)$. Moreover, if $\tilde{\kappa}(0) = 1$, then Bochner’s theorem guarantees that $\rho(\omega)$ is a normalized density function, i.e.

$$\tilde{\kappa}(q - k) = \int_{\mathbb{R}^d} \rho(\omega) \exp(i\omega^T (q - k)) d\omega = \mathbb{E}_{\omega \sim \rho} [\exp(i\omega^T q) \exp(i\omega^T k)^*]. \quad (2)$$

Rahimi & Recht (2007) proposed to sample from the spectral density $\rho(\omega)$ for a Monte Carlo approximation to the integral in Eq. (2). Specifically, for real valued kernels, they define $\kappa(q, k) \approx \phi(q)^T \phi(k)$, where $\omega_i \sim \rho(\omega)$ and

$$\phi(x) := \text{RKS}(x, \Omega = (\omega_1, \dots, \omega_M)) := \frac{1}{\sqrt{M}} [\cos(\omega_1^T x), \dots, \cos(\omega_M^T x), \sin(\omega_1^T x), \dots, \sin(\omega_M^T x)] \quad (3)$$

To learn a kernel, we can either learn a parametric function $\kappa(\cdot, \cdot)$ or learn the corresponding parameterized feature map $\phi(\cdot)$ directly, which corresponds to learning the spectral density $\rho(\omega)$ (Wilson & Adams, 2013; Yang et al., 2015; Oliva et al., 2016). In this paper, we focus on the latter because this helps us in keeping the computational complexity linear in the sequence length L . This can be achieved by rewriting Eq. (1) as $\text{ATTN}(X)_i = \frac{\phi(q_i)^T (\sum_{j=1}^L \phi(k_j) v_j^T)}{\phi(q_i)^T \sum_{j'=1}^L \phi(k_{j'})}$. To the best of our knowledge this is the first attempt to learn the kernel of the generalized self-attention mechanism (Eq. 1).

2.1 Learning Kernels in Spectral Domain

GMM-RKS: Our objective is to enable learning of any translation invariant kernel. This is realizable if we can learn the spectral distribution. Gaussian Mixture Models (GMMs) are known universal approximators of densities and hence may approximate any spectral distribution. GMMs have been shown to be useful for kernel learning for regression and classification tasks (Wilson & Adams, 2013; Oliva et al., 2016). Thus, to learn the kernel of the generalized self-attention mechanism (Eq. 1), we model the spectral distribution of the kernel as a parameterized GMM, i.e.

$$\rho(\omega) = \sum_{c=1}^C \pi_c \mathcal{N}(\mu_c, \Sigma_c) \Leftrightarrow \kappa(q, k) = \sum_{c=1}^C \pi_c e^{(i\mu_c^T (q-k) - \frac{1}{2}(q-k)^T \Sigma_c (q-k))} \quad (4)$$

Here $\{\mu_c \in \mathbb{R}^d, \Sigma_c \in \mathbb{R}^{d^2}\}_{c=1}^C$ are the learnable parameters of the feature map and C is the number of components in the Gaussian mixture. It can be shown using Plancherel’s Theorem that $\rho(\omega)$ can approximate any shift invariant kernel (Silverman, 1986). Since we are working with only real valued kernels, the corresponding kernel reduces to $\kappa(q, k) = \sum_{c=1}^C \pi_c e^{(-\frac{1}{2}(q-k)^T \Sigma_c (q-k))} \cos(\mu_c^T (q - k))$.

To speedup learning, we assume that $\pi_c = \frac{1}{C}$ and parameterize the feature map with spectral frequency, $\Omega = (\omega_{c,1}, \dots, \omega_{c,M})$ as:

$$\phi_{\text{GMM-RKS}}(x) := \text{RKS}(x, \Omega), \quad \omega_{c,m} = \Sigma_c n_m + \mu_c, \quad n_m \sim \mathcal{N}(\mathbf{0}, \mathbf{I}). \quad (5)$$

This allows us to sample $n_m \sim \mathcal{N}(\mathbf{0}, \mathbf{I})$ and learn the parameters of the feature map, $(\{\mu_c \in \mathbb{R}^{d_q}, \Sigma_c \in \mathbb{R}^{d_q^2}\}_{c=1}^C)$ end-to-end along with the other parameters of the Transformer.

FASTFOOD-RKS: GMM-RKS removes the quadratic dependency on context length, but we still need to calculate $\Omega^T \mathbf{Q}$ and $\Omega^T \mathbf{K}$ (where $\Omega = [\omega_1, \omega_2, \dots, \omega_M]$) which takes $\mathcal{O}(Md_qL)$ time and $\mathcal{O}(Md_q + d_qL + ML)$ space, which can be too much if M is large. For further gains in scalability, we approximate the spectral frequency matrix Ω , using the product of Hadamard matrices (FastFood; Le et al., 2013), such that the computation can be done in time log-linear in M , i.e.:

$$\phi_{\text{FASTFOOD-RKS}}(x) := \text{RKS}(x, V), \quad \text{where } V = \frac{1}{\sigma \sqrt{d_q}} SHG\Pi HB. \quad (6)$$

Here, $\Pi \in \{0, 1\}^{d_q \times d_q}$ is a permutation matrix, H is the Walsh-Hadamard matrix, B is a diagonal random matrix with $\{\pm 1\}$ entries, G is a diagonal matrix with Gaussian entries drawn from $\mathcal{N}(0, 1)$ and finally S is a random diagonal scaling matrix that makes the row lengths non-uniform. The entire multiplication can be carried out in logarithmic time, and the space requirement is reduced by storing diagonal matrices instead of full matrices. For $M > d_q$ we use multiple blocks, and the only restriction is that we need $M|d_q$. In order to make this learnable, Yang et al. (2015) proposed making S and optionally G and B learnable. For the main paper, we keep all three learnable (the case where only S is learnable is discussed in Appendix D).

GENERATIVE-RKS: If we increase the number of components (C) in GMM-RKS, the computation and space complexity increases dramatically. Instead, to learn a more generic kernel, without blowing up the computational complexity, we use deep generative models (DGMs). DGMs have achieved impressive results in density estimation (Goodfellow et al., 2014; Kingma & Welling, 2014; Richardson & Weiss, 2018; Ruthotto & Haber, 2021) and end-to-end kernel learning in the spectral domain for classification (Fang et al., 2020).

In GENERATIVE-RKS we use a DGM to replace the Gaussian probability distribution from GMM-RKS with an arbitrary probability distribution. This DGM acts as a generator similar to the ones used by variational auto-encoders used in computer vision (Kingma & Welling, 2014). In particular, to make the sampling process differentiable, we use the reparameterization trick, where a learnable neural network (called the generator, and denoted by g in Figure 2) transforms samples from a simple noise distribution (ρ_0 in Fig 2) into samples from the desired distribution.

$$\omega_m = g(n_m), \quad n_m \sim \rho_0(\cdot) \quad (7)$$

The generator network is trained end to end with the whole model, allowing it to choose the best possible distribution for the given data. These samples ($\Omega = [\omega_1, \omega_2, \dots, \omega_M]$ in Fig 2) are then used in Random Kitchen Sinks as follows:

$$\phi_{\text{GENERATIVE-RKS}}(x) := \text{RKS}(x, \Omega), \quad \omega_m \sim g(\rho_0) \quad (8)$$

We experimented with various configurations and eventually chose to learn a generator network which consisted of 4 fully connected layers with batch normalisation and LeakyReLU activation, followed by a single fully connected layer with tanh activation. While this methodology allows us to generalise the gaussian distribution to a much larger class of distributions, it also causes a blowup in the number of parameters e.g. a $4 + 1$ layer constant width generator, as used by us would require $5d^2 + 5d$ parameters as opposed to the $d^2 + d$ parameters in GMM-RKS. To counter this and to improve generalization, we share the same generator network across all heads in a layer, which means that the different heads only differ in the Query/Key/Value projection matrix.

Positive Random Features (PRF): Until now, we focused on feature maps defined using RKS. While our formulation is very general, recently it was shown that positive random features provide a better approximation to both Gaussian and Softmax kernels (see Lemma 2 in Choromanski et al. 2021b). In particular they showed that $\kappa(q, k) = \exp(q^T k) = \mathbb{E}_{\omega \sim \mathcal{N}(0, I)} [\exp(\omega^T q - \frac{\|q\|^2}{2}) \exp(\omega^T k - \frac{\|k\|^2}{2})]$ and demonstrated that Monte Carlo approximation to this expectation leads to a low variance estimate of the softmax kernel. Moreover, the presence of only positive values within the randomized feature map ensures that kernel estimates remain strictly non-negative. To incorporate this prior knowledge, we propose a novel kernel learning framework in which we learn the spectral density while using the feature map corresponding to the above expectation. For instance, when we model the spectral distribution of $\Omega = (\omega_1, \dots, \omega_M)$ using GMM ($\psi = \sum_{c=1}^C \pi_c \mathcal{N}(\mu_c, \Sigma_c)$) we have that:

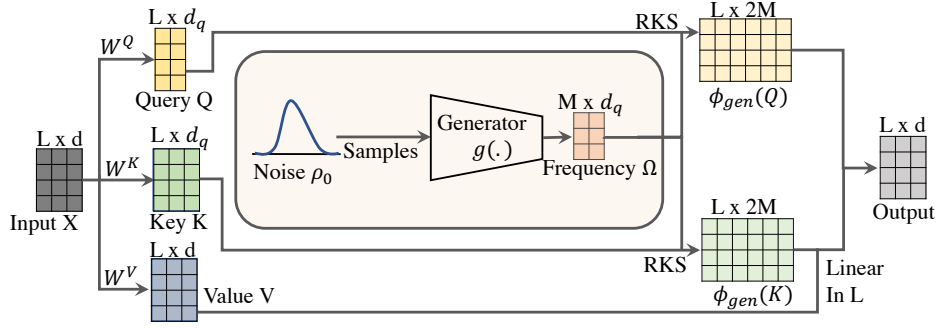


Figure 2: Generalized self-attention with deep generative RKS. Q , V and K are linear transformations of input, X . The generator generates spectral frequency (Ω) from an implicit spectral distribution. Using RKS (Eq. 2) we create the feature map ϕ_{gen} (Eq. 8). The numerator of the output is calculated as $\phi_{gen}(Q)(\phi_{gen}(K)V)$ while the denominator is $\phi_{gen}(q_i)^T \sum_{j'=1}^L \phi_{gen}(k_{j'})$ making attention linear in sequence length L .

Model	Space Complexity	Time Complexity
Softmax Transformer	$\mathcal{O}(L^2(1 + d_q/L))$	$\mathcal{O}(L^2 d_q)$
Performer	$\mathcal{O}(L(d_q + M + Md_q/L))$	$\mathcal{O}(LMd_q)$
LinearElu	$\mathcal{O}(L(d_q + d_q^2/L))$	$\mathcal{O}(Ld_q^2)$
GMM-RKS	$\mathcal{O}(L(d_q + C(d_q^2/L + Md_q/L + M)))$	$\mathcal{O}(MC(d_q^2 + Ld_q))$
GMM-PRF	$\mathcal{O}(L(d_q + CMd_q/L + CM))$	$\mathcal{O}(LCMd_q)$
FASTFOOD(RKS/PRF)	$\mathcal{O}(L(d_q + M + Md_q/L))$	$\mathcal{O}(LMd_q)$
GENERATIVE(RKS/PRF)	$\mathcal{O}(L(d_q + d_q^2/L + Md_q/L + M))$	$\mathcal{O}(M(d_q^2 + Ld_q))$

Table 1: Space and time complexity of self-attention kernel of KL-TRANSFORMERS compared with Softmax Transformer (Vaswani et al., 2017), Performer (Choromanski et al., 2021b), and LinearElu (Katharopoulos et al., 2020). L refers to length of context, $d_q=d_v$ is the query/key/value dimension, while M is the number of samples (where applicable).

$$\kappa(q, k) := \mathbb{E}_{\omega \sim \psi} [e^{(\omega^T q - \|q\|^2)} e^{(\omega^T k - \|k\|^2)}], \quad PRF(x, \Omega) := \frac{e^{-\|x\|^2}}{\sqrt{M}} [e^{\omega_1^T x}, \dots, e^{\omega_M^T x}] \quad (9)$$

$$\phi_{\text{GMM-PRF}}(x) := PRF(x, (\omega_{c,1}, \dots, \omega_{c,M})), \quad \omega_{c,m} = \sum_c n_m + \mu_c, \quad n_m \sim \mathcal{N}(\mathbf{0}, \mathbf{I}) \quad (10)$$

Similarly we redefine the other two methods as:

$$\phi_{\text{GENERATIVE-PRF}}(x) := PRF(x, \Omega), \quad \omega_m = g(n_m), \quad n_m \sim \rho_o(\cdot) \quad (11)$$

$$\phi_{\text{FASTFOOD-PRF}}(x) := PRF(x, V), \quad \text{where } V = \frac{1}{\sigma \sqrt{d_q}} SHGIIHB. \quad (12)$$

To the best of our knowledge we are the first to explore kernel learning with positive random features.

2.2 Analysis

In this section, we explore what can be said about the expressivity of the proposed linear time KL-TRANSFORMERS. While our understanding of the properties of Transformers is rudimentary, we would still like to know whether the known properties extend to our models. For example, it has been shown that Softmax Transformers and its sparse counterparts are Turing complete (Pérez et al., 2019; Zaheer et al., 2020). This raises the question as to whether the proposed linear KL-TRANSFORMERS are also Turing complete?

It is easy to see that the generalized kernel self-attention (Eq. 1) includes the softmax kernel and hence should satisfy the properties of Softmax Transformer. Interestingly, we can also show that this property holds for GMM-RKS Transformers with number of components $C = 1$, (for a more systematic definition, see Section A.1). More formally,

Theorem 1: *The class of GMM-RKS Transformers with positional embeddings is Turing complete.*

Proof is in the Appendix A. We also show that:

Theorem 2: *The class of GMM-PRF Transformers with positional embeddings is Turing complete.*

For a detailed proof, see Appendix A.

Since the sampling of ω in Equations 5 and 9 is random, we have some stochasticity in the attention layers of our model. We now show that the Mean Square Error (MSE) of the estimation can be reduced by reducing the eigenvalues of the learnt covariance matrix. In particular, we show that:

Theorem 3: *Let μ and $\Sigma = S^T S$ be the learnt mean and covariance matrices of the sampling distribution. Further let q and k be the parameters, and $p = k - q$ and $o = k + q$ be their vector difference and sum respectively, and m be the number of samples. The MSE of the linear approximations is given by:*

$$MSE_{\text{GMM-RKS}} = \frac{2}{m} \cos^2(\mu^T p) (1 - e^{-\|S^T p\|^2})^2 \quad (13)$$

$$MSE_{\text{GMM-PRF}} = \frac{1}{m} e^{-2(\|q\|^2 + \|k\|^2 - \mu^T o)} (e^{2\|S^T o\|} - e^{\|S^T o\|}) \quad (14)$$

It is interesting to note that in this formulation, $MSE_{\text{GMM-RKS}}^2$ is bounded above by $\frac{2}{m}$ while no such bound can be established for $MSE_{\text{GMM-PRF}}$. For the detailed proof see Supplementary Section B

Complexity Analysis: While all of our models have linear complexity with respect to the context length L , differences still exist amongst the various methods. Notable, GMM-RKS and GENERATIVE have quadratic time and space complexity in the query size d_q . Both the FASTFOOD methods avoid this approximation, whereas GMM-PRF avoids this by the use of a diagonal covariance matrix. The complexities are listed in Table 1.

Another factor that controls timing is the sampling of Ω . Sampling too frequently can lead to significant slowdowns whereas sampling too few times can lead to biased learning. For our experiments, we resample every 100 training iterations, although this can be changed. A detailed list of all hyperparameters along with implementation details are provided in Appendix C.

3 Experiments

3.1 Does kernel learning improve performance of fixed kernel methods on longer sequences?

Long Range Arena (*LRA*; Tay et al. 2021b) is a diverse benchmark for the purpose of evaluating the ability of sequence models to reason under long-context scenarios. It includes tasks that vary both in terms of the context length (ranging from $1K$ to $4K$ tokens) as well as the data modalities (including text and mathematical expressions). We evaluate the KL-TRANSFORMER architectures introduced in Section 2.1 on the *Text*, *Retrieval* and *ListOps* tasks from *LRA* which deal with sentiment prediction from IMDB Reviews, document similarity classification and pre-order arithmetic calculations respectively. Both *Text* and *Retrieval* use character level encodings, bringing their maximum length to 4000 tokens. The *ListOps* dataset is synthetically generated and has a fixed length of 2000 tokens. For more details on the tasks, we refer the interested reader to the original paper by Tay et al. 2021b.

Setup: To ensure a fair comparison, we closely follow the same data preprocessing, data split, model size and training procedure as in (Tay et al., 2021b). Within each task, a common configuration is used across all KL-TRANSFORMER

²For the proof of Theorem 3, we use the specific case of $C = 2$, $\mu_1 + \mu_2 = 0$ and $\Sigma_1 = \Sigma_2$ which is used in the experiments. Since Theorem 1 and 2 however, hold in general

Model	Complexity	ListOps	Text	Retrieval	Avg.
		2K	4K	4K	
Random Predictor	NA	10.00	50.00	50.00	36.67
Baseline Models					
Softmax Trans. (Vaswani et al.)	$\mathcal{O}(L^2)$	36.38	64.27	57.46	52.70
Synthesizer (Tay et al.)	$\mathcal{O}(L^2)$	36.50	61.68	54.67	50.95
Sinkhorn (Tay et al.)	$\mathcal{O}((L/B)^2)$	34.20	61.20	53.83	49.74
Sparse Trans. (Child et al.)	$\mathcal{O}(L\sqrt{L})$	35.78	63.58	59.59	52.98
Reformer (Kitaev et al.)	$\mathcal{O}(L \log L)$	36.30	56.10	53.40	48.60
Local Attention (Parmar et al.)	$\mathcal{O}(LK)$	15.95	52.98	53.39	40.77
Longformer (Beltagy et al.)	$\mathcal{O}(LK)$	36.03	62.85	56.89	51.92
Linformer (Wang et al.)	$\mathcal{O}(L)$	35.49	53.49	52.27	52.56
Big Bird (Zaheer et al.)	$\mathcal{O}(LK)$	37.08	64.02	59.29	53.46
LinearElu (Katharopoulos et al.)	$\mathcal{O}(L)$	17.15	65.90	53.09	45.38
Performer (Choromanski et al.)	$\mathcal{O}(L)$	36.00	65.40	53.82	51.74
Kernelized Transformers					
GMM-RKS (Eq. 5)	$\mathcal{O}(L)$	18.55	63.95	58.64	47.05
FASTFOOD-RKS (Eq. 6)	$\mathcal{O}(L)$	18.65	<u>65.67</u>	61.92	48.75
GENERATIVE-RKS (Eq. 8)	$\mathcal{O}(L)$	18.50	66.50	64.76	49.92
GMM-PRF (Eqs. 9, 10)	$\mathcal{O}(L)$	36.96	62.64	65.27	54.96
FASTFOOD-PRF (Eqs. 9, 12)	$\mathcal{O}(L)$	<u>37.05</u>	64.66	71.13	57.61
GENERATIVE-PRF (Eqs. 9, 11)	$\mathcal{O}(L)$	37.42	62.90	69.81	<u>56.71</u>

Table 2: Experimental results on the *LRA* benchmark. We report accuracy on the test set, except for *Text* where validation set is used. The best model is in boldface and the second best is underlined if within 1% of the best. Accuracy scores for all baseline models are from Tay et al. (2021b). Here, L refers to the sequence length, K refers to the size of a local window and $B \ll L$ is a model specific parameter. For our models, accuracy is averaged over 100 runs.

models based on the configuration specified in the *LRA* code repository³. We outline the hyperparameters for all tasks in Table 6 in the Appendix.

Results: The results across all *LRA* tasks are summarized in Table 2. KL-TRANSFORMER variants that learn the kernel function directly from the data in an end-to-end manner outperform the baseline models by occupying both best and second-best performances. We find that KL-TRANSFORMERS based on PRFs tend to outperform their RKS counterparts which is also reflected on the average *LRA* score, with FASTFOOD-PRF being the best-performing model.

3.2 Trade-off between Accuracy and Efficiency

We benchmark the efficiency of each KL-TRANSFORMER in terms of peak memory usage and training speed and compare it against three baseline models from the *LRA* benchmark. Specifically, we compare against other efficient Transformer architectures that employ fixed kernel feature maps (e.g. LinearElu and Performer) as well as the Softmax Transformer which is one of the strongest baseline models (see Table 2). We conduct efficiency benchmarks on the two *LRA* tasks with sequence length equal to $4K$ in order to assess the efficiency of these methods in modelling tasks that require a long context (results for the other two datasets are included in the Appendix). Speed measurements (steps per second) refer to wall-clock training time (including overheads). In both cases experiments are conducted on 8 NVIDIA TITAN RTX GPUs. The comparison is illustrated in Figure 3. On the *Text* task, GENERATIVE-RKS is the best performing model, although it consumes more memory than the remaining KL-TRANSFORMER architectures (it is still more efficient than the Softmax Transformer). LinearElu consumes the least amount of memory, while GMM-RKS provides a trade-off between the two. In *Retrieval* the situation is much clearer, with FASTFOOD-PRF and GENERATIVE-PRF outperforming significantly other models in terms of accuracy while having very low memory

³<https://github.com/google-research/long-range-arena>

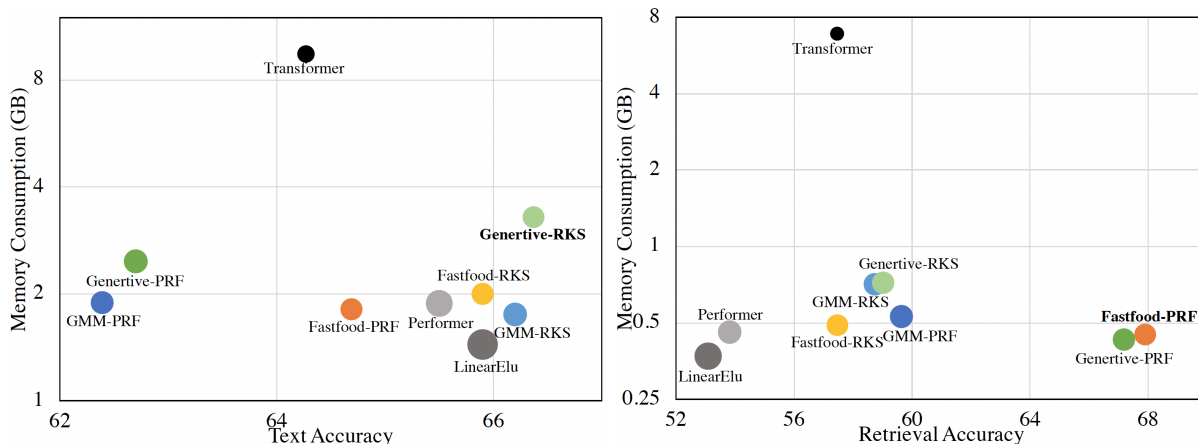


Figure 3: We compare the peak memory consumption (y-axis), performance (x-axis) and speed (denoted by area of circle) for the various KL-TRANSFORMER architectures on the two *LRA* tasks with sequence length equal to $4K$. Memory usage refers to average memory usage across GPUs and speed (steps per second) for each model is reported relative to the speed of Softmax Transformer (larger circles denote faster models). For a similar graph on the *ListOps* Task see Fig 8 in the Supplementary

consumption. The training speed of KL-TRANSFORMERS is of the same order of magnitude as Performers (as indicated by the area of each circle in Figure 3).

Lastly, in Figure 4, we report the peak memory consumption as the sequence length changes from $1K$ to $4K$ on the *Text* dataset. As expected, all our models have a linear increase in memory consumption with increasing sequence length, as opposed to the Softmax Transformer which has dramatic increase in memory consumption. Furthermore, Figure 7 in the Appendix reports the memory usage of each KL-TRANSFORMER across all datasets. We find that FASTFOOD-PRF and GENERATIVE-PRF are not only our best performing models on average, but they also consume the least memory among various KL-TRANSFORMERS across all datasets. Thus, among the models proposed in this paper, we can recommend FASTFOOD-PRF and GENERATIVE-PRF as the model that achieves the best accuracy with the least memory consumption.

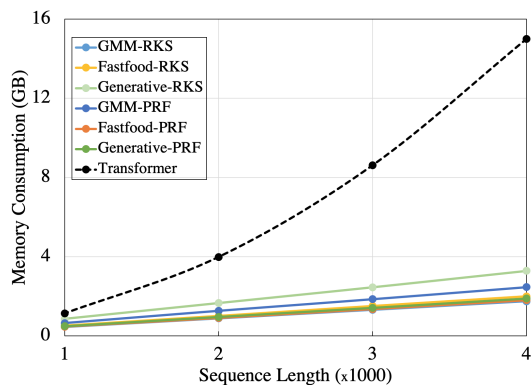


Figure 4: Memory vs sequence length

3.3 How do KL-TRANSFORMERS perform on short sequence tasks?

We compare the KL-TRANSFORMERS and Softmax Transformer in a common transfer learning setting. We adopt the setting of BERT-like models (Devlin et al., 2019; Liu et al., 2019), except that we have fewer layers and heads (see Table 8 for details) and pre-train all models (including Softmax Transformer) on the WikiText-103 dataset (Merity et al., 2016) using non-contextual WordPiece embeddings (Wu et al., 2016). Pre-trained models are then fine-tuned on the General Language Understanding Evaluation (*GLUE*) benchmark (Wang et al., 2019), a collection of resources for training and evaluating language understanding systems. All tasks in *GLUE* consist of either one or two sentences as input and can therefore be easily captured with a context of size 512. Since the context length is rather short, the difference between training and inference time across the various models is minimal. Instead, the main goal of this task is to assess how do KL-TRANSFORMERS compare against Softmax Transformers on a set of tasks where the later have been established as the *de-facto* architecture.

The results on all downstream *GLUE* tasks are shown in Table 3. Crucially, we demonstrate that there is no significant loss in performance compared to Softmax Transformers when kernelized variants are used on short language modelling tasks. As illustrated in Table 3, KL-TRANSFORMERS perform on par with the Softmax Transformer.

Model	SST2 (acc)	MRPC (acc/f1)	QQP (acc/f1)	MNLI- m/mm (acc/acc)	QNLI (acc)	WNLI (acc)	RTE (acc)	CoLA (MCor)
Softmax Trans.	0.81	0.70/0.82	0.83/0.76	0.64/0.64	0.68	0.56	0.6	0.18
FASTFOOD-RKS	0.83	0.71/0.82	0.81/0.74	0.57/0.57	0.64	0.59	0.56	0.13
GMM-RKS	0.80	0.70/0.82	0.77/0.69	0.47/0.48	0.60	0.61	0.57	0.07
GENERATIVE-RKS	0.81	0.70/0.82	0.81/0.73	0.59/0.58	0.63	0.62	0.58	0.16
FASTFOOD-PRF	0.81	0.71/0.82	0.81/0.74	0.56/0.57	0.64	0.59	0.58	0.12
GENERATIVE-PRF	0.80	0.71/0.82	0.80/0.74	0.56/0.56	0.61	0.60	0.55	0.10
GMM-PRF	0.82	0.71/0.82	0.81/0.74	0.56/0.56	0.64	0.59	0.59	0.21

Table 3: Results on the GLUE benchmark after fine-tuning on respective tasks. KL-TRANSFORMERS continue to be competitive to Transformers even in short context problems.

Task	Model	Max Egv.	Mean Egv.	Task	Model	Max Egv.	Mean Egv.
Text	GMM-RKS	0.486	0.031	Retrieval	GMM-RKS	0.499	0.053
	GMM-PRF	0.096	0.025		GMM-PRF	0.186	0.042

Table 4: Distribution of Eigenvalues for GMM-RKS and GMM-PRF models for the *Text* and *Retrieval* tasks. For a head by head distribution see Tables 9, 10, 11 and 12

4 Empirical Analysis

In section 3, we observed that our models compare favourably with other linear models, with Positive Random Features (PRF) based models usually doing better than the ones based on Random Kitchen Sinks (RKS) (although RKS does better on the *Text* task). In this section, we want to compare these linear kernels in terms of their empirical variance and how well they deal with sparsity. In Theorem 3, we already noted that the MSE for both GMM-RKS and GMM-PRF models decreases with decrease in eigenvalues of the covariance matrices, making it useful to learn such a matrix. We also noted that the variance in the output of GMM-RKS is bounded, and thus it should not face issues with sparse datasets when approximating the softmax kernel as shown in Choromanski et al. (2021b)). We test for these results empirically in subsections 4.1 and 4.2 respectively. We then conclude in 4.3 with a discussion on which of our proposed models is best to use in a given scenario.

4.1 Comparison of variance

Looking at the eigenvalues of the covariance matrices of our final trained models⁴ in Table 4, we find that GMM-RKS and GMM-PRF models trained on the *Text* and *Retrieval* tasks indeed learn to have eigenvalues significantly smaller than 1 (which would be the case for non-learnable co-variances).

While lower eigenvalues reduce the variance in our models significantly, it does not get completely nullified. To understand how much stochastic remains in our models, and also to compare RKS with PRF in regards to their variance, we look at the final outputs⁵ the models produce when repeatedly run on the same example. We record the output produced by the model for 100 runs on each datapoint, and calculate the following 3 metrics to quantify the variance:

- 1. Relative Standard Deviation (RSD):** RSD is a standardised measure of dispersion (see Currie & Svehla (1994), def 3.9), defined as the ratio of the standard deviation of a set of observations to the absolute value of their mean. The ratio ensures that the measure is invariant to scaling (eg. multiplying the penultimate layer of the model by a constant factor does not affect RSD) while the absolute of the mean ensures that opposing classes don't cancel each other out.

⁴We only report eigenvalues for the GMM models since covariance matrices are not well defined in the Generator and FastFood. Also, the *ListOps* task is left out of the entire analysis because its multi-class nature makes the analysis complex

⁵While the theory makes a claim about the output of each attention head, evaluating every head at every layer would give us a large number of values to analyse. The output is considered before applying the final sigmoid

2. **Prediction Inconsistency (PI):** While RSD quantifies the variance in the model’s continuous output, in practice, only the sign of the output is of interest as that decides the predicted class. As a way to quantify stochasticity in the discrete output, we count the number of times the output does not have the majority label, i.e., if the output is positive x times, then we have $PI = \min(x, 100 - x)$. Alternately, it can be seen as the failure rate if we treat the majority prediction as the true class.
3. **Accuracy Gain with Voting (AGV):** Since the final output has a propensity to change its sign, we can get a more robust prediction at inference time by running the model multiple times and considering the class it predicts more times as its output, instead of taking the prediction from a single inference step. Doing so, we are likely to get closer to the mean prediction (by the Law of Large Numbers, see Révész et al. (2014)), and we get accuracy scores which are slightly higher than those reported in Table 2, and we call this value the *Voting Accuracy (VA)*. AGV is then defined as the ratio between the voting accuracy and the regular accuracy.

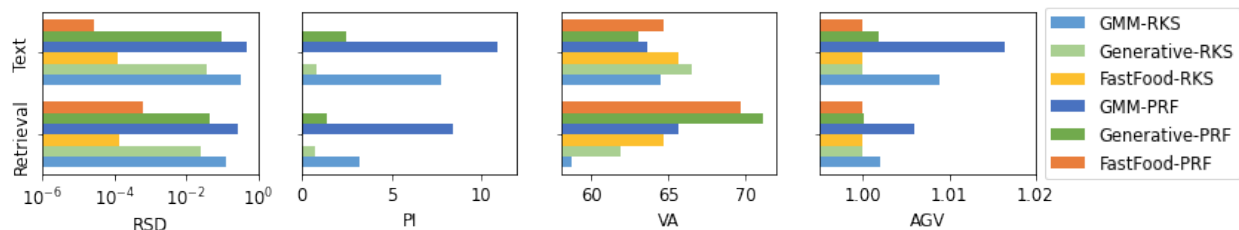


Figure 5: Values of variance metrics Relative Standard Deviation (RSD), Prediction Inconsistency(PI), Average Gain with Voting (AGV) as well as Voting Accuracy (VA) on the *Text* and *Retrieval* tasks.

The above metrics, in addition to the *Voting Accuracy*, are calculated over all instances in the validation and test set for *Text* and *Retrieval* tasks respectively, and plotted in Fig. 5. We note that our 3 metrics are all highly correlated with each other (R^2 values 0.95, 0.98 and 0.89 for RSD-AGV, RSD-PI and AGV-PI respectively, see supplementary Fig 9, 10).

We notice that our RKS based models, in general, have lower variance as compared to our PRF models. We also note that Generator and FastFood are able to further reduce the variance in the output, possibly due to additional learnable parameters in Generator and fewer sources of randomness in FastFood. We also notice that all models have greater variance in the *Text* task, and it is possible that this is related to the better performance of RKS based models in this task, and their inherent lower variance helps them outperform their PRF counterparts.

4.2 Effectiveness on Sparse Datasets

Choromanski et al. (2021b) demonstrated that if Random Kitchen Sinks are used to estimate the softmax-kernel, the MSE tends to ∞ as the raw softmax scores tend to 0. This makes it particularly hard to deal with sparse datasets where multiple positions need near-zero attention.

Thus, in order to test how sparsity in the dataset affects our models, we design a synthetic experiment where the model is fed a sequence of ordered pairs, where the first element, which we call *score*, takes a value of -1 or 1 , and the second element, which we call *relevance*, takes a value of 0 or 1 . Looking at the sequence, the model must predict the sum of the scores at all positions with relevance $= 1$. Note that any position with relevance $= 0$ does not contribute to the final answer, and therefore, does not need to be attended to. We construct the inputs by sampling the relevance of each position from Bernoulli(p). Thus, the sparsity can be controlled by changing p (for a detailed description of the task, see Supplementary).

Figure 6 shows the learning curves for various sparsity levels in our synthetic experiment. Due to the simple nature of the task, all models eventually reach 100% accuracy. We observe that

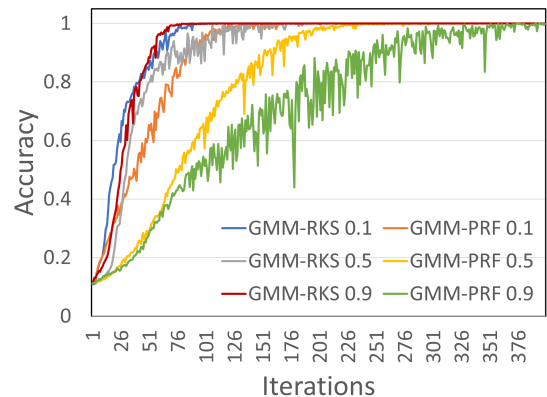


Figure 6: Learning curves for our synthetic experiment. The number after the model name is inversely proportional to sparsity in the dataset

the convergence time of GMM-RKS remains more or less unchanged with increasing sparsity, while for GMM-PRF the model converges slower as sparsity decreases. We believe that the slower convergence of GMM-PRF is correlated to the variance in its output, which leads to variance in gradients. Observing the gradients propagated to the classifier layer (See Table 14 in Supplementary), we find that this is indeed the case, and not only is the variance in the gradients higher for GMM-PRF, but also the mean is higher, making it take bigger steps in an uncertain direction. This result provides us an insight into which models to use under which circumstances.

4.3 Which Model to Use?

PRF outperforms RKS in terms of accuracy in most of our experiments, especially if we are able to run multiple inference steps. Therefore, in general, we recommend using PRF over RKS. However, if consistency of predictions is important, or rapid training is required on a not-so-sparse task, one may consider RKS as well.

Finally, we observe that Generator and Fastfood methods always outperform the vanilla linearisations. Between them, Fastfood can be significantly faster if properly implemented on GPU. However, generators may perform better if a large amount of data is available since they provide a greater amount of flexibility.

5 Related Work

5.1 Efficient Transformers

A wide variety of approaches belong to the class of efficient Transformers (Tay et al., 2020b). We survey them below:

Sparse models: Memory Compressed Transformer (Liu et al., 2018) uses a convolution kernel (of size K) to subsample keys and values reducing the complexity to $\mathcal{O}(L^2K^{-1})$. Inspired by the notion of sparsity, Child et al. (2019) introduced sparse factorizations of the attention matrix to reduce the overall complexity to $\mathcal{O}(L\sqrt{L})$. Subsequently, Roy et al. (2020) proposed the Routing Transformer which employs K -means clustering to learn dynamic sparse attention regions, achieving an overall complexity of $\mathcal{O}(L\sqrt{L})$. Recently, Sun et al. (2022) proposed yet another sparse $\mathcal{O}(L\sqrt{L})$ approach that learns which bucket each query/key is to be placed in based on final attention values. Sparsity has also been achieved by efficiently subsampling queries and/or keys (Chen et al., 2021). Kitaev et al. (2020) proposed the Reformer, which reduces complexity to $\mathcal{O}(L \log L)$ by using locality-sensitive hashing to group together similar symbols. Ye et al. (2019) also proposed a $\mathcal{O}(L \log L)$ algorithm using binary partitions of data. There also exist other works that mainly focus on memory reduction (Liu et al., 2018; Tay et al., 2020a; Gupta et al., 2021). While these methods are faster than Softmax Transformers, their asymptotic time complexity remains quadratic. Further approaches attempt to minimize the constants involved in the quadratic attention, but keep the same asymptotic complexity (Dutta et al., 2021; Chen et al., 2022).

Local or Global Attention: Parmar et al. (2018) was one of the first local attention models that achieved $\mathcal{O}(L)$ complexity in both time and space, by using local attention over a constant length-context. A similar local attention based method was also utilized by Zhang et al. (2021) and Liu et al. (2022), the latter of which added special tokens at the start of each local attention block, which attend globally. Another set of methods proposed to approximate the global attention by replacing the softmax to allow changing the order of matrix multiplication, making the calculation of the QKV product linear in the context length (Yorsh et al., 2021; Hua et al., 2022; Qin et al., 2022). Linearised global attention is also used by Performer (Choromanski et al., 2021b), which has been built upon by other works. Chen (2021) and Luo et al. (2021) both try to improve the performance of Performer by incorporating relative positional embeddings which they show makes it strictly stronger in terms of representability. Choromanski et al. (2021a) tries to combine RKS and PRF attentions by a learnable weight parameter to get the best of both worlds. Both these methods can be applied as is to our work. Schlag et al. (2021a) take a different view on this, claiming that having stochasticity hampers performance, and propose a deterministic feature map to avoid this.

Multiple Types of Attention: Beltagy et al. (2020) proposed a $\mathcal{O}(L)$ method that combines the above two approaches by using local sliding windows as well as global attention components. Zaheer et al. (2020) proposed Big Bird, another sparse attention mechanism which combines global attention, random attention and local attention to reduce the complexity to $\mathcal{O}(L)$. A similar construction was previously used by Ainslie et al. (2020). More recently the combination of global and local attention has been utilized by Zhu et al. (2021) and Nguyen et al. (2021). Further, Xiong et al. (2021) adapted the Nyström method to approximate standard self-attention with $\mathcal{O}(L)$ complexity. Lu et al. (2021) also makes

use of a similar near-field and far-field attention mechanism, where the far field attention is calculated via a low rank approximation using \tanh and $ReLU$ non-linearities. A different line of work has attempted to limit the number of key-value pairs that are to be attended to, by attempting to summarise the variable length context with a fixed number of memory-cells (Zhang & Cai, 2022; Ma et al., 2021). While some of these more nuanced approaches outperform KL-TRANSFORMER, most of their innovations are orthogonal to ours, and none of these approaches explore kernel learning within the attention mechanism of Transformers.

5.2 Kernel Learning

While kernel methods have long been used to solve non-linear statistical problems, they traditionally scaled poorly with the number of data points thereby limiting their applicability on large datasets (Vapnik et al., 1997; Cortes & Vapnik, 1995; Schölkopf et al., 1998; Schölkopf & Smola, 2001; Hofmann et al., 2008). Prior to RKS, several kernel approximation techniques have been proposed to improve the scalability of kernel methods, including greedy basis selection techniques (Smola & Schölkopf, 2000), divide-and-conquer approaches (Hsieh et al., 2014; Zhang et al., 2013; Liu et al., 2020), non-stationary spectral kernels (Remes et al., 2017), generalized spectral kernels (Samo & Roberts, 2015) as well as Nyström methods (Williams & Seeger, 2001).

The method of Random Kitchen Sinks has been revisited several times, either to improve the approximation quality (Yu et al., 2016b; Choromanski et al., 2017; Li, 2017; Avron et al., 2016; Lyu, 2017), reduce the time and memory complexity (Le et al., 2013; Choromanski & Sindhwani, 2016; Feng et al., 2015; Dao et al., 2017) or analyze theoretically the risk and generalization properties of the algorithm (Sutherland & Schneider, 2015; Sun et al., 2018; Li et al., 2019b). A systematic survey of random feature methods for approximating kernel functions can be found in (Liu et al., 2021).

Lastly, there exist a class of methods that extend the RKS framework to enable kernel learning. Representative approaches involve either a one-stage (Yang et al., 2015; Fang et al., 2020) or a two-stage procedure (Sinha & Duchi, 2016; Li et al., 2019a; Bullins et al., 2018; Shen et al., 2019). Two-stage approaches involve an intermediate step in which the problem of kernel-alignment is solved (Cristianini et al., 2002). However, solving the kernel-alignment problem requires accessed to labeled data which is not available in this case, as inputs to the kernel learning algorithm are the intermediate representations of the input sequence.

6 Conclusion

In this paper, we bridged the gap between advances in kernel learning and efficient Transformers by proposing several kernel learning methods for Transformers that increase the expressiveness of Transformers while keeping the computational complexity linear in sequence length. We showed that our proposed KL-TRANSFORMER are Turing-complete and can control their variance. Experimentally our proposed models perform on par with, and possibly exceed the performance of existing efficient transformer architectures on long context tasks without falling behind on short context tasks. We also found that for some datasets such as *ListOps*, RKS based models tend to fall short of their PRF counterparts. Our experiments further demonstrate that the memory consumption of our models scales linearly with the sequence length.

Ethical Considerations

Our work is on making Transformers computationally efficient without losing expressiveness. Our models were evaluated on publicly available benchmark datasets. The datasets used in our work do not contain sensitive information to the best of our knowledge.

Reproducibility: We plan to open source the entire code of the KL-TRANSFORMER framework (including the implementation of all models as well as the code for replicating all of our experiments) before the camera ready version of the paper. As part of this submission, we include code for all the methods proposed by us along with instructions on how to reproduce results. A detailed description of all hyperparameters (for both *LRA* as well as *GLUE* benchmarks) has been included in Appendix C. Finally, regarding our theoretical contributions, we present a detailed theoretical analysis in Appendix A.

References

- Milton Abramowitz and Irene A Stegun. Handbook of mathematical functions with formulas, graphs, and mathematical tables. national bureau of standards applied mathematics series 55. tenth printing. 1972.
- Joshua Ainslie, Santiago Ontañón, Chris Alberti, Philip Pham, Anirudh Ravula, and Sumit Sanghai. ETC: encoding long and structured data in transformers. *CoRR*, abs/2004.08483, 2020.
- Haim Avron, Vikas Sindhwani, Jiyang Yang, and Michael W. Mahoney. Quasi-monte carlo feature maps for shift-invariant kernels. *Journal of Machine Learning Research*, 17(120):1–38, 2016.
- Iz Beltagy, Matthew E. Peters, and Arman Cohan. Longformer: The long-document transformer, 2020.
- Tom Brown, Benjamin Mann, Nick Ryder, Melanie Subbiah, Jared D Kaplan, Prafulla Dhariwal, Arvind Neelakantan, Pranav Shyam, Girish Sastry, Amanda Askell, Sandhini Agarwal, Ariel Herbert-Voss, Gretchen Krueger, Tom Henighan, Rewon Child, Aditya Ramesh, Daniel Ziegler, Jeffrey Wu, Clemens Winter, Chris Hesse, Mark Chen, Eric Sigler, Mateusz Litwin, Scott Gray, Benjamin Chess, Jack Clark, Christopher Berner, Sam McCandlish, Alec Radford, Ilya Sutskever, and Dario Amodei. Language models are few-shot learners. In H. Larochelle, M. Ranzato, R. Hadsell, M. F. Balcan, and H. Lin (eds.), *Advances in Neural Information Processing Systems*, volume 33, pp. 1877–1901. Curran Associates, Inc., 2020.
- Brian Bullins, Cyril Zhang, and Yi Zhang. Not-so-random features. In *International Conference on Learning Representations*, 2018.
- Nicolas Carion, Francisco Massa, Gabriel Synnaeve, Nicolas Usunier, Alexander Kirillov, and Sergey Zagoruyko. End-to-end object detection with transformers, 2020.
- Peng Chen. Permuteformer: Efficient relative position encoding for long sequences, 2021. URL <https://arxiv.org/abs/2109.02377>.
- Yifan Chen, Qi Zeng, Dilek Hakkani-Tur, Di Jin, Heng Ji, and Yun Yang. Sketching as a tool for understanding and accelerating self-attention for long sequences, 2021.
- Zhaodong Chen, Yuying Quan, Zheng Qu, Liu Liu, Yufei Ding, and Yuan Xie. Dynamic n:m fine-grained structured sparse attention mechanism, 2022. URL <https://arxiv.org/abs/2203.00091>.
- Rewon Child, Scott Gray, Alec Radford, and Ilya Sutskever. Generating long sequences with sparse transformers, 2019.
- Krzysztof Choromanski and Vikas Sindhwani. Recycling randomness with structure for sublinear time kernel expansions. In *Proceedings of the 33rd International Conference on International Conference on Machine Learning - Volume 48*, ICML'16, pp. 2502–2510. JMLR.org, 2016.
- Krzysztof Choromanski, Haoxian Chen, Han Lin, Yuanzhe Ma, Arijit Sehanobish, Deepali Jain, Michael S. Ryoo, Jake Varley, Andy Zeng, Valerii Likhoshesterov, Dmitry Kalashnikov, Vikas Sindhwani, and Adrian Weller. Hybrid random features. *CoRR*, abs/2110.04367, 2021a. URL <https://arxiv.org/abs/2110.04367>.
- Krzysztof M Choromanski, Mark Rowland, and Adrian Weller. The unreasonable effectiveness of structured random orthogonal embeddings. In I. Guyon, U. V. Luxburg, S. Bengio, H. Wallach, R. Fergus, S. Vishwanathan, and R. Garnett (eds.), *Advances in Neural Information Processing Systems*, volume 30. Curran Associates, Inc., 2017.
- Krzysztof Marcin Choromanski, Valerii Likhoshesterov, David Dohan, Xingyou Song, Andreea Gane, Tamas Sarlos, Peter Hawkins, Jared Quincy Davis, Afroz Mohiuddin, Lukasz Kaiser, David Benjamin Belanger, Lucy J Colwell, and Adrian Weller. Rethinking attention with performers. In *International Conference on Learning Representations*, 2021b.
- Corinna Cortes and Vladimir Vapnik. Support-vector networks. *Mach. Learn.*, 20(3):273–297, September 1995. ISSN 0885-6125. doi: 10.1023/A:1022627411411.
- Nello Cristianini, John Shawe-Taylor, André Elisseeff, and Jaz Kandola. On kernel-target alignment. In T. Dietterich, S. Becker, and Z. Ghahramani (eds.), *Advances in Neural Information Processing Systems*, volume 14. MIT Press, 2002.

- L. A. Currie and G. Svehla. Nomenclature for the presentation of results of chemical analysis (iupac recommendations 1994). *Pure and Applied Chemistry*, 66(3):595–608, 1994. doi: doi:10.1351/pac199466030595. URL <https://doi.org/10.1351/pac199466030595>.
- Tri Dao, Christopher M De Sa, and Christopher Ré. Gaussian quadrature for kernel features. In I. Guyon, U. V. Luxburg, S. Bengio, H. Wallach, R. Fergus, S. Vishwanathan, and R. Garnett (eds.), *Advances in Neural Information Processing Systems*, volume 30. Curran Associates, Inc., 2017.
- Jacob Devlin, Ming-Wei Chang, Kenton Lee, and Kristina Toutanova. BERT: Pre-training of deep bidirectional transformers for language understanding. In *Proceedings of the 2019 Conference of the North American Chapter of the Association for Computational Linguistics: Human Language Technologies, Volume 1 (Long and Short Papers)*, pp. 4171–4186, Minneapolis, Minnesota, June 2019. Association for Computational Linguistics. doi: 10.18653/v1/N19-1423.
- Subhabrata Dutta, Tanya Gautam, Soumen Chakrabarti, and Tanmoy Chakraborty. Redesigning the transformer architecture with insights from multi-particle dynamical systems. In M. Ranzato, A. Beygelzimer, Y. Dauphin, P.S. Liang, and J. Wortman Vaughan (eds.), *Advances in Neural Information Processing Systems*, volume 34, pp. 5531–5544. Curran Associates, Inc., 2021. URL <https://proceedings.neurips.cc/paper/2021/file/2bd388f731f26312bfc0fe30da009595-Paper.pdf>.
- Kun Fang, Xiaolin Huang, Fanghui Liu, and Jie Yang. End-to-end kernel learning via generative random fourier features, 2020.
- Chang Feng, Qinghua Hu, and Shizhong Liao. Random feature mapping with signed circulant matrix projection. In *Proceedings of the 24th International Conference on Artificial Intelligence, IJCAI'15*, pp. 3490–3496. AAAI Press, 2015. ISBN 9781577357384.
- Ian Goodfellow, Jean Pouget-Abadie, Mehdi Mirza, Bing Xu, David Warde-Farley, Sherjil Ozair, Aaron Courville, and Yoshua Bengio. Generative adversarial nets. In Z. Ghahramani, M. Welling, C. Cortes, N. Lawrence, and K. Q. Weinberger (eds.), *Advances in Neural Information Processing Systems*, volume 27. Curran Associates, Inc., 2014.
- Ankit Gupta, Guy Dar, Shaya Goodman, David Ciprut, and Jonathan Berant. Memory-efficient transformers via top- k attention, 2021. URL <https://arxiv.org/abs/2106.06899>.
- Thomas Hofmann, Bernhard Schölkopf, and Alexander J. Smola. Kernel methods in machine learning. *The Annals of Statistics*, 36(3):1171 – 1220, 2008. doi: 10.1214/009053607000000677.
- Cho-Jui Hsieh, Si Si, and Inderjit S. Dhillon. A divide-and-conquer solver for kernel support vector machines. In *Proceedings of the 31st International Conference on International Conference on Machine Learning - Volume 32, ICML'14*, pp. I-566–I-574. JMLR.org, 2014.
- Weizhe Hua, Zihang Dai, Hanxiao Liu, and Quoc V. Le. Transformer quality in linear time, 2022. URL <https://arxiv.org/abs/2202.10447>.
- John Ingraham, Vikas Garg, Regina Barzilay, and Tommi Jaakkola. Generative models for graph-based protein design. In H. Wallach, H. Larochelle, A. Beygelzimer, E. Fox, and R. Garnett (eds.), *Advances in Neural Information Processing Systems*, volume 32, pp. 15820–15831. Curran Associates, Inc., 2019.
- Angelos Katharopoulos, Apoorv Vyas, Nikolaos Pappas, and François Fleuret. Transformers are RNNs: Fast autoregressive transformers with linear attention. In Hal Daumé III and Aarti Singh (eds.), *Proceedings of the 37th International Conference on Machine Learning*, volume 119 of *Proceedings of Machine Learning Research*, pp. 5156–5165. PMLR, 13–18 Jul 2020.
- Diederik P Kingma and Max Welling. Auto-encoding variational bayes, 2014.
- Nikita Kitaev, Lukasz Kaiser, and Anselm Levskaya. Reformer: The efficient transformer. In *International Conference on Learning Representations*, 2020.
- Alex Krizhevsky. Learning multiple layers of features from tiny images. Technical report, 2009.

- Quoc Le, Tamas Sarlos, and Alexander Smola. Fastfood - computing hilbert space expansions in loglinear time. In Sanjoy Dasgupta and David McAllester (eds.), *Proceedings of the 30th International Conference on Machine Learning*, volume 28 of *Proceedings of Machine Learning Research*, pp. 244–252, Atlanta, Georgia, USA, 17–19 Jun 2013. PMLR.
- Chun-Liang Li, Wei-Cheng Chang, Youssef Mroueh, Yiming Yang, and Barnabas Poczos. Implicit kernel learning. In Kamalika Chaudhuri and Masashi Sugiyama (eds.), *Proceedings of Machine Learning Research*, volume 89 of *Proceedings of Machine Learning Research*, pp. 2007–2016. PMLR, 16–18 Apr 2019a.
- Ping Li. Linearized gmm kernels and normalized random fourier features. In *Proceedings of the 23rd ACM SIGKDD International Conference on Knowledge Discovery and Data Mining, KDD '17*, pp. 315–324, New York, NY, USA, 2017. Association for Computing Machinery. ISBN 9781450348874. doi: 10.1145/3097983.3098081.
- Zhu Li, Jean-Francois Ton, Dino Ogljic, and Dino Sejdinovic. Towards a unified analysis of random Fourier features. In Kamalika Chaudhuri and Ruslan Salakhutdinov (eds.), *Proceedings of the 36th International Conference on Machine Learning*, volume 97 of *Proceedings of Machine Learning Research*, pp. 3905–3914. PMLR, 09–15 Jun 2019b.
- Fanghui Liu, Xiaolin Huang, Chen Gong, Jie Yang, and Li Li. Learning data-adaptive non-parametric kernels. *Journal of Machine Learning Research*, 21(208):1–39, 2020.
- Fanghui Liu, Xiaolin Huang, Yudong Chen, and Johan A. K. Suykens. Random features for kernel approximation: A survey on algorithms, theory, and beyond, 2021.
- Peter J. Liu, Mohammad Saleh, Etienne Pot, Ben Goodrich, Ryan Sepassi, Lukasz Kaiser, and Noam Shazeer. Generating wikipedia by summarizing long sequences. In *International Conference on Learning Representations*, 2018.
- Yang Liu, Jiayang Liu, Li Chen, Yuxiang Lu, Shikun Feng, Zhida Feng, Yu Sun, Hao Tian, Hua Wu, and Haifeng Wang. Ernie-sparse: Learning hierarchical efficient transformer through regularized self-attention, 2022. URL <https://arxiv.org/abs/2203.12276>.
- Yinhan Liu, Myle Ott, Naman Goyal, Jingfei Du, Mandar Joshi, Danqi Chen, Omer Levy, Mike Lewis, Luke Zettlemoyer, and Veselin Stoyanov. Roberta: A robustly optimized bert pretraining approach, 2019.
- Jiachen Lu, Jinghan Yao, Junge Zhang, Xiatian Zhu, Hang Xu, Weiguo Gao, Chunjing Xu, Tao Xiang, and Li Zhang. Soft: Softmax-free transformer with linear complexity, 2021.
- Jiasen Lu, Dhruv Batra, Devi Parikh, and Stefan Lee. Vilbert: Pretraining task-agnostic visiolinguistic representations for vision-and-language tasks. In H. Wallach, H. Larochelle, A. Beygelzimer, E. Fox, and R. Garnett (eds.), *Advances in Neural Information Processing Systems*, volume 32, pp. 13–23. Curran Associates, Inc., 2019.
- Shengjie Luo, Shanda Li, Tianle Cai, Di He, Dinglan Peng, Shuxin Zheng, Guolin Ke, Liwei Wang, and Tie-Yan Liu. Stable, fast and accurate: Kernelized attention with relative positional encoding, 2021. URL <https://arxiv.org/abs/2106.12566>.
- Yueming Lyu. Spherical structured feature maps for kernel approximation. In Doina Precup and Yee Whye Teh (eds.), *Proceedings of the 34th International Conference on Machine Learning*, volume 70 of *Proceedings of Machine Learning Research*, pp. 2256–2264. PMLR, 06–11 Aug 2017.
- Xuezhe Ma, Xiang Kong, Sinong Wang, Chunting Zhou, Jonathan May, Hao Ma, and Luke Zettlemoyer. Luna: Linear unified nested attention. In M. Ranzato, A. Beygelzimer, Y. Dauphin, P.S. Liang, and J. Wortman Vaughan (eds.), *Advances in Neural Information Processing Systems*, volume 34, pp. 2441–2453. Curran Associates, Inc., 2021. URL <https://proceedings.neurips.cc/paper/2021/file/14319d9cfc6123106878dc20b94fbaf3-Paper.pdf>.
- Ali Madani, Bryan McCann, Nikhil Naik, Nitish Shirish Keskar, Namrata Anand, Raphael R. Eguchi, Po-Ssu Huang, and Richard Socher. Progen: Language modeling for protein generation, 2020.
- Stephen Merity, Caiming Xiong, James Bradbury, and Richard Socher. Pointer sentinel mixture models, 2016.

- Tan Nguyen, Vai Suliafu, Stanley Osher, Long Chen, and Bao Wang. Fmmformer: Efficient and flexible transformer via decomposed near-field and far-field attention. In M. Ranzato, A. Beygelzimer, Y. Dauphin, P.S. Liang, and J. Wortman Vaughan (eds.), *Advances in Neural Information Processing Systems*, volume 34, pp. 29449–29463. Curran Associates, Inc., 2021. URL <https://proceedings.neurips.cc/paper/2021/file/f621585df244e9596dc70a39b579efb1-Paper.pdf>.
- Junier B. Oliva, Avinava Dubey, Andrew G. Wilson, Barnabas Poczos, Jeff Schneider, and Eric P. Xing. Bayesian nonparametric kernel-learning. In Arthur Gretton and Christian C. Robert (eds.), *Proceedings of the 19th International Conference on Artificial Intelligence and Statistics*, volume 51 of *Proceedings of Machine Learning Research*, pp. 1078–1086, Cadiz, Spain, 09–11 May 2016. PMLR.
- Niki Parmar, Ashish Vaswani, Jakob Uszkoreit, Lukasz Kaiser, Noam Shazeer, Alexander Ku, and Dustin Tran. Image transformer. In Jennifer Dy and Andreas Krause (eds.), *Proceedings of the 35th International Conference on Machine Learning*, volume 80 of *Proceedings of Machine Learning Research*, pp. 4055–4064, Stockholmsmässan, Stockholm Sweden, 10–15 Jul 2018. PMLR.
- Adam Paszke, Sam Gross, Francisco Massa, Adam Lerer, James Bradbury, Gregory Chanan, Trevor Killeen, Zeming Lin, Natalia Gimelshein, Luca Antiga, Alban Desmaison, Andreas Kopf, Edward Yang, Zachary DeVito, Martin Raison, Alykhan Tejani, Sasank Chilamkurthy, Benoit Steiner, Lu Fang, Junjie Bai, and Soumith Chintala. Pytorch: An imperative style, high-performance deep learning library. In H. Wallach, H. Larochelle, A. Beygelzimer, F. d'Alché-Buc, E. Fox, and R. Garnett (eds.), *Advances in Neural Information Processing Systems*, volume 32. Curran Associates, Inc., 2019.
- Hao Peng, Nikolaos Pappas, Dani Yogatama, Roy Schwartz, Noah A. Smith, and Lingpeng Kong. Random feature attention. *CoRR*, abs/2103.02143, 2021.
- Jorge Pérez, Javier Marinkovic, and Pablo Barceló. On the turing completeness of modern neural network architectures. *CoRR*, abs/1901.03429, 2019.
- Jorge Pérez, Javier Marinković, and Pablo Barceló. On the turing completeness of modern neural network architectures. In *International Conference on Learning Representations*, 2019.
- Zhen Qin, Weixuan Sun, Hui Deng, Dongxu Li, Yunshen Wei, Baohong Lv, Junjie Yan, Lingpeng Kong, and Yiran Zhong. cosformer: Rethinking softmax in attention, 2022.
- Alec Radford, Karthik Narasimhan, Tim Salimans, and Ilya Sutskever. Improving language understanding by generative pre-training, 2018.
- Colin Raffel, Noam Shazeer, Adam Roberts, Katherine Lee, Sharan Narang, Michael Matena, Yanqi Zhou, Wei Li, and Peter J. Liu. Exploring the limits of transfer learning with a unified text-to-text transformer. *Journal of Machine Learning Research*, 21(140):1–67, 2020.
- Ali Rahimi and Benjamin Recht. Random features for large-scale kernel machines. In *Proceedings of the 20th International Conference on Neural Information Processing Systems*, NIPS'07, pp. 1177–1184, Red Hook, NY, USA, 2007. Curran Associates Inc. ISBN 9781605603520.
- Sami Remes, Markus Heinonen, and Samuel Kaski. Non-stationary spectral kernels. In I. Guyon, U. V. Luxburg, S. Bengio, H. Wallach, R. Fergus, S. Vishwanathan, and R. Garnett (eds.), *Advances in Neural Information Processing Systems*, volume 30. Curran Associates, Inc., 2017.
- P. Révész, Z.W. Birnbaum, and E. Lukacs. *The Laws of Large Numbers*. Probability and mathematical statistics. Elsevier Science, 2014. ISBN 9781483269023. URL <https://books.google.ch/books?id=ochiBQAAQBAJ>.
- Eitan Richardson and Yair Weiss. On gans and gmms. In S. Bengio, H. Wallach, H. Larochelle, K. Grauman, N. Cesa-Bianchi, and R. Garnett (eds.), *Advances in Neural Information Processing Systems*, volume 31. Curran Associates, Inc., 2018.
- Alexander Rives, Joshua Meier, Tom Sercu, Siddharth Goyal, Zeming Lin, Demi Guo, Myle Ott, C. Lawrence Zitnick, Jerry Ma, and Rob Fergus. Biological structure and function emerge from scaling unsupervised learning to 250 million protein sequences. *bioRxiv*, 2020. doi: 10.1101/622803.

- Aurko Roy, Mohammad Saffar, Ashish Vaswani, and David Grangier. Efficient content-based sparse attention with routing transformers, 2020.
- Walter Rudin. *Fourier Analysis on Groups*. John Wiley & Sons, Ltd, 1990.
- Lars Ruthotto and Eldad Haber. An introduction to deep generative modeling, 2021.
- Yves-Laurent Kom Samo and Stephen Roberts. Generalized spectral kernels, 2015.
- Imanol Schlag, Kazuki Irie, and Jürgen Schmidhuber. Linear transformers are secretly fast weight programmers. In Marina Meila and Tong Zhang (eds.), *Proceedings of the 38th International Conference on Machine Learning*, volume 139 of *Proceedings of Machine Learning Research*, pp. 9355–9366. PMLR, 18–24 Jul 2021a. URL <https://proceedings.mlr.press/v139/schlag21a.html>.
- Imanol Schlag, Kazuki Irie, and Jürgen Schmidhuber. Linear transformers are secretly fast weight programmers. In Marina Meila and Tong Zhang (eds.), *Proceedings of the 38th International Conference on Machine Learning*, volume 139 of *Proceedings of Machine Learning Research*, pp. 9355–9366. PMLR, 18–24 Jul 2021b.
- Bernhard Schölkopf and Alexander J. Smola. *Learning with Kernels: Support Vector Machines, Regularization, Optimization, and Beyond*. MIT Press, Cambridge, MA, USA, 2001. ISBN 0262194759.
- Bernhard Schölkopf, Alexander Smola, and Klaus-Robert Müller. Nonlinear component analysis as a kernel eigenvalue problem. *Neural Computation*, 10(5):1299–1319, 1998. doi: 10.1162/089976698300017467.
- Zheyang Shen, Markus Heinonen, and Samuel Kaski. Harmonizable mixture kernels with variational fourier features. In Kamalika Chaudhuri and Masashi Sugiyama (eds.), *Proceedings of the Twenty-Second International Conference on Artificial Intelligence and Statistics*, volume 89 of *Proceedings of Machine Learning Research*, pp. 3273–3282. PMLR, 16–18 Apr 2019.
- Bernard W Silverman. *Density estimation for statistics and data analysis*, volume 26. CRC press, 1986.
- Aman Sinha and John C Duchi. Learning kernels with random features. In D. Lee, M. Sugiyama, U. Luxburg, I. Guyon, and R. Garnett (eds.), *Advances in Neural Information Processing Systems*, volume 29. Curran Associates, Inc., 2016.
- Alex J. Smola and Bernhard Schölkopf. Sparse greedy matrix approximation for machine learning. In *Proceedings of the Seventeenth International Conference on Machine Learning*, ICML ’00, pp. 911–918, San Francisco, CA, USA, 2000. Morgan Kaufmann Publishers Inc. ISBN 1558607072.
- Yitong Sun, Anna Gilbert, and Ambuj Tewari. But how does it work in theory? linear svm with random features. In S. Bengio, H. Wallach, H. Larochelle, K. Grauman, N. Cesa-Bianchi, and R. Garnett (eds.), *Advances in Neural Information Processing Systems*, volume 31. Curran Associates, Inc., 2018.
- Zhiqing Sun, Yiming Yang, and Shinjae Yoo. Sparse attention with learning to hash. In *International Conference on Learning Representations*, 2022. URL <https://openreview.net/forum?id=VGnOJhd5Q1q>.
- Dougal J. Sutherland and Jeff Schneider. On the error of random fourier features. In *Proceedings of the Thirty-First Conference on Uncertainty in Artificial Intelligence*, UAI’15, pp. 862–871, Arlington, Virginia, USA, 2015. AUAI Press. ISBN 9780996643108.
- Yi Tay, Dara Bahri, Liu Yang, Donald Metzler, and Da-Cheng Juan. Sparse sinkhorn attention. In Hal Daumé III and Aarti Singh (eds.), *Proceedings of the 37th International Conference on Machine Learning*, volume 119 of *Proceedings of Machine Learning Research*, pp. 9438–9447. PMLR, 13–18 Jul 2020a.
- Yi Tay, Mostafa Dehghani, Dara Bahri, and Donald Metzler. Efficient transformers: A survey, 2020b.
- Yi Tay, Dara Bahri, Donald Metzler, Da-Cheng Juan, Zhe Zhao, and Che Zheng. Synthesizer: Rethinking self-attention in transformer models, 2021a.
- Yi Tay, Mostafa Dehghani, Samira Abnar, Yikang Shen, Dara Bahri, Philip Pham, Jinfeng Rao, Liu Yang, Sebastian Ruder, and Donald Metzler. Long range arena : A benchmark for efficient transformers. In *International Conference on Learning Representations*, 2021b.

- Yao-Hung Hubert Tsai, Shaojie Bai, Makoto Yamada, Louis-Philippe Morency, and Ruslan Salakhutdinov. Transformer dissection: An unified understanding for transformer’s attention via the lens of kernel. In *Proceedings of the 2019 Conference on Empirical Methods in Natural Language Processing and the 9th International Joint Conference on Natural Language Processing (EMNLP-IJCNLP)*, pp. 4344–4353, Hong Kong, China, November 2019. Association for Computational Linguistics. doi: 10.18653/v1/D19-1443.
- Vladimir Vapnik, Steven Golowich, and Alex Smola. Support vector method for function approximation, regression estimation and signal processing. In M. C. Mozer, M. Jordan, and T. Petsche (eds.), *Advances in Neural Information Processing Systems*, volume 9. MIT Press, 1997.
- Ashish Vaswani, Noam Shazeer, Niki Parmar, Jakob Uszkoreit, Llion Jones, Aidan N Gomez, Łukasz Kaiser, and Illia Polosukhin. Attention is all you need. In I. Guyon, U. V. Luxburg, S. Bengio, H. Wallach, R. Fergus, S. Vishwanathan, and R. Garnett (eds.), *Advances in Neural Information Processing Systems*, volume 30, pp. 5998–6008. Curran Associates, Inc., 2017.
- Alex Wang, Amanpreet Singh, Julian Michael, Felix Hill, Omer Levy, and Samuel R. Bowman. GLUE: A multi-task benchmark and analysis platform for natural language understanding. In *International Conference on Learning Representations*, 2019.
- Sinong Wang, Belinda Z. Li, Madian Khabsa, Han Fang, and Hao Ma. Linformer: Self-attention with linear complexity, 2020.
- Christopher Williams and Matthias Seeger. Using the nyström method to speed up kernel machines. In T. Leen, T. Dietterich, and V. Tresp (eds.), *Advances in Neural Information Processing Systems*, volume 13. MIT Press, 2001.
- Andrew Wilson and Ryan Adams. Gaussian process kernels for pattern discovery and extrapolation. In Sanjoy Dasgupta and David McAllester (eds.), *Proceedings of the 30th International Conference on Machine Learning*, volume 28 of *Proceedings of Machine Learning Research*, pp. 1067–1075, Atlanta, Georgia, USA, 17–19 Jun 2013. PMLR.
- Yonghui Wu, Mike Schuster, Zhifeng Chen, Quoc V. Le, Mohammad Norouzi, Wolfgang Macherey, Maxim Krikun, Yuan Cao, Qin Gao, Klaus Macherey, Jeff Klingner, Apurva Shah, Melvin Johnson, Xiaobing Liu, Łukasz Kaiser, Stephan Gouws, Yoshikiyo Kato, Taku Kudo, Hideto Kazawa, Keith Stevens, George Kurian, Nishant Patil, Wei Wang, Cliff Young, Jason Smith, Jason Riesa, Alex Rudnick, Oriol Vinyals, Greg Corrado, Macduff Hughes, and Jeffrey Dean. Google’s neural machine translation system: Bridging the gap between human and machine translation, 2016.
- Yunyang Xiong, Zhanpeng Zeng, Rudrasis Chakraborty, Mingxing Tan, Glenn Fung, Yin Li, and Vikas Singh. Nyströmformer: A nyström-based algorithm for approximating self-attention. *Proceedings of the AAAI Conference on Artificial Intelligence*, 35(16):14138–14148, May 2021.
- Zichao Yang, Andrew Wilson, Alex Smola, and Le Song. A la Carte – Learning Fast Kernels. In Guy Lebanon and S. V. N. Vishwanathan (eds.), *Proceedings of the Eighteenth International Conference on Artificial Intelligence and Statistics*, volume 38 of *Proceedings of Machine Learning Research*, pp. 1098–1106, San Diego, California, USA, 09–12 May 2015. PMLR.
- Zihao Ye, Qipeng Guo, Quan Gan, Xipeng Qiu, and Zheng Zhang. Bp-transformer: Modelling long-range context via binary partitioning, 2019.
- Uladzislau Yorsh, Pavel Kordik, and Alexander Kovalenko. Simpletron: Eliminating softmax from attention computation, 2021. URL <https://arxiv.org/abs/2111.15588>.
- Felix Xinnan X Yu, Ananda Theertha Suresh, Krzysztof M Choromanski, Daniel N Holtmann-Rice, and Sanjiv Kumar. Orthogonal random features. In D. Lee, M. Sugiyama, U. Luxburg, I. Guyon, and R. Garnett (eds.), *Advances in Neural Information Processing Systems*, volume 29. Curran Associates, Inc., 2016a. URL <https://proceedings.neurips.cc/paper/2016/file/53adaf494dc89ef7196d73636eb2451b-Paper.pdf>.
- Felix Xinnan X Yu, Ananda Theertha Suresh, Krzysztof M Choromanski, Daniel N Holtmann-Rice, and Sanjiv Kumar. Orthogonal random features. In D. Lee, M. Sugiyama, U. Luxburg, I. Guyon, and R. Garnett (eds.), *Advances in Neural Information Processing Systems*, volume 29. Curran Associates, Inc., 2016b.

- Manzil Zaheer, Guru Guruganesh, Kumar Avinava Dubey, Joshua Ainslie, Chris Alberti, Santiago Ontanon, Philip Pham, Anirudh Ravula, Qifan Wang, Li Yang, and Amr Ahmed. Big bird: Transformers for longer sequences. In H. Larochelle, M. Ranzato, R. Hadsell, M. F. Balcan, and H. Lin (eds.), *Advances in Neural Information Processing Systems*, volume 33, pp. 17283–17297. Curran Associates, Inc., 2020.
- Hang Zhang, Yeyun Gong, Yelong Shen, Weisheng Li, Jiancheng Lv, Nan Duan, and Weizhu Chen. Poolingformer: Long document modeling with pooling attention. In Marina Meila and Tong Zhang (eds.), *Proceedings of the 38th International Conference on Machine Learning*, volume 139 of *Proceedings of Machine Learning Research*, pp. 12437–12446. PMLR, 18–24 Jul 2021. URL <https://proceedings.mlr.press/v139/zhang21h.html>.
- Yizhe Zhang and Deng Cai. Linearizing transformer with key-value memory, 2022.
- Yuchen Zhang, John Duchi, and Martin Wainwright. Divide and conquer kernel ridge regression. In Shai Shalev-Shwartz and Ingo Steinwart (eds.), *Proceedings of the 26th Annual Conference on Learning Theory*, volume 30 of *Proceedings of Machine Learning Research*, pp. 592–617, Princeton, NJ, USA, 12–14 Jun 2013. PMLR.
- Chen Zhu, Wei Ping, Chaowei Xiao, Mohammad Shoeybi, Tom Goldstein, Anima Anandkumar, and Bryan Catanzaro. Long-short transformer: Efficient transformers for language and vision. In M. Ranzato, A. Beygelzimer, Y. Dauphin, P.S. Liang, and J. Wortman Vaughan (eds.), *Advances in Neural Information Processing Systems*, volume 34, pp. 17723–17736. Curran Associates, Inc., 2021. URL <https://proceedings.neurips.cc/paper/2021/file/9425be43ba92c2b4454ca7bf602efad8-Paper.pdf>.

Learning The Transformer Kernel – Appendix

A Detailed proof of Theorems

A.1 Definitions

Transformer: A transformer consists of an Encoder and a Decoder, which in turn consist of several encoder and decoder layers respectively. A single encoder layer consists of an attention layer (Att) and a 2 layer feed-forward neural network (O):

$$\mathbf{a}_i = Att(W_q \mathbf{x}_i, W_k \mathbf{X}, W_v \mathbf{X}) + \mathbf{x}_i \quad (15)$$

$$\mathbf{z}_i = O(\mathbf{a}_i) + \mathbf{a}_i \quad (16)$$

In our case, the feed-forward neural network uses perceptron activations (ie $f_{perc}(x) = 1$ iff $x > 0$ and 0 otherwise) and the attention is gaussian (discussed in detail later). The final layer of the encoder is followed by a couple of two layer output neural networks, which produce the Encoder Key (\mathbf{K}_e) and Encoder Value (\mathbf{V}_e) to be used by the decoder. In our proof, we assume these to have ReLU activation ($f_{ReLU}(x) = \max(0, x)$)

The decoder layers are similar to the encoder layer except for an additional cross attention layer which attends to the encoder output:

$$\mathbf{p}_i = Att(W_q \mathbf{y}_i, W_k \mathbf{Y}, W_v \mathbf{Y}) + \mathbf{y}_i \quad (17)$$

$$\mathbf{a}_i = Att(W'_q \mathbf{p}_i, \mathbf{K}_e, \mathbf{V}_e) + \mathbf{y}_i \quad (18)$$

$$\mathbf{z}_i = O(\mathbf{a}_i) + \mathbf{a}_i \quad (19)$$

Unlike the encoder, the decoder self attention in Eq. 17 can only attend to previous position. After the final layer we have a two layer feed-forward neural network with ReLU activation to produce the output. The decoder is initialised with a special *seed vector* and is repeatedly applied with the right shifted output of the last application as the input of the current application, until some termination condition is fulfilled.

Both the encoder and decoder can further use *position embeddings*, which have the same dimension as the output of each layer, and are added to the input prior to the first layer. These help in establishing the order of the input

Since the output of any unit of a layer is independent of values to its right, these do not change with time and can be cached. The output of the final layer of the rightmost cell can therefore be regarded as the model state encoding (v)

Turing Machine: A Turing Machine is an abstract construct which consists of a right infinite tape and a read-write head. Each cell of the tape can hold one of many symbols from a predefined alphabet Σ which includes a special blank symbol b . Additionally, the read-write head can be in one of many possible states within the state-space Q which includes a special initial state q_{init} and a subset of final states F .

Initially, the tape contains the input followed by an infinite number of blank symbols, while the head starts off in the last non-blank cell. In each step, the head executes in accordance with a transition function $T(s^{(i)}, q^{(i)}) = (v^{(i)}, q^{(i+1)}, m^{(i)})$, ie, based on the symbol currently under the head and the current state, it decides the symbol it wants to overwrite the current symbol with, the state it will be in the next step and the direction it wants to move, which can be either left(-1) or right(1). We assume that the transition function already makes sure that the head never moves left from the leftmost cell.

For the purpose of our proof, we additionally define $c^{(i)}$ as the index of the cell to which the head currently points, $\ell(i)$, which represents the step number when the head last pointed to the current cell, ie $\ell(i) = \max\{j | c^{(j)} = c^{(i)}\}$. In the special case where the current cell is being visited for the first time, we have $\ell(i) = i - 1$

A.2 The Proof

In this section, we provide a general proof which works for both **Theorem 1** and **Theorem 2** in the paper. This is possible since the construction only makes use of the dual of the kernel functions used, i.e. the gaussian. The fact that

both kernel functions map to the gaussian is shown in lemma S.2 (Sec A.6)

Our proof is based on the similar proof in Pérez et al. (2019). Any symbols not explicitly defined have same meanings from that paper. We begin the proof by defining our model encoding(\mathbf{v}):

$$\mathbf{v} = [\mathbf{q}_1, \mathbf{s}_1, x_1, x_2, \mathbf{q}_2, \mathbf{s}_2, x_3, x_4, x_5, x_6, x_7, \mathbf{s}_4, x_8, x_9, x_{10}, x_{11}, x_{12}] \quad (20)$$

where $q_i \in \mathbb{Q}^{|Q|}$, $s_i \in \mathbb{Q}^{|\Sigma|}$, and $x_i \in \mathbb{Q}$, giving a total model size of $2|Q| + 3|\Sigma| + 14$. Hereafter, $\llbracket x \rrbracket$ represents the one-hot encoding for the state x or symbol x depending on the position it is being used in. $\mathbf{0}_q$ represents all 0's in a state field, and represents the q_{copy} state discussed later, while $\mathbf{0}_s$ represents all 0's in a symbol field, and represents the blank symbol. Further, $\beta^{(i)} = \min(i, n)$ where n is the size of the encoder and $\alpha^{(i)}$ represents the symbol at position $\beta^{(i)}$ in the encoder. We assume that atleast the last cell of the encoder contains a blank symbol.

This differs from Pérez et al. (2019) in the addition of a fourth scalar in the first group, in which we intend to store the current position $c^{(i)}$ of the head.

Our invariant is that \mathbf{y}_i the output from the decoder at timestep i , stores:

1. The current state of the Turing Machine($q^{(i)}$)
2. The symbol under the head($s^{(i)}$)
3. The direction of movement of the head in the previous timestep ($m^{(i-1)}$)
4. The current position of the head($c^{(i)}$)

In all, we get $\mathbf{y}_i = [\llbracket q^{(i)} \rrbracket, \llbracket s^{(i)} \rrbracket, m^{(i-1)}, c^{(i)}, 0, \dots, 0]$

Positional Embeddings: The last group ($x_9, x_{10}, x_{11}, x_{12}$) is dedicated to the positional embeddings, which are given as $(1, i, \frac{1}{i}, \frac{1}{i^2})$. These same embeddings are added on both the Encoder and Decoder side.

Encoder: The encoder consists of a single layer. It gets as input the symbol at position i and the positional embeddings, ie $input_i = [\mathbf{0}_q, \mathbf{0}_s, 0, 0, \mathbf{0}_q, \llbracket s^{(i)} \rrbracket, 0, 0, 0, 0, i, \mathbf{0}_s, 0, 1, i, \frac{1}{i}, \frac{1}{i^2}]$ which has a trivial attention layer (ie, one that outputs all zeroes) and a feed forward layer which separates the positional embeddings from the symbols, giving $\mathbf{k}_i^e = [0, \dots, 0, i, -1, 0, 0]$ and $\mathbf{v}_i^e = [\mathbf{0}_q, \mathbf{0}_s, 0, 0, \mathbf{0}_q, \llbracket s^{(i)} \rrbracket, 0, 0, 0, 0, i, \mathbf{0}_s, 0, 0, 0, 0, 0]$.

Decoder Layer 1: The first layer of the decoder calculates the next state, the symbol to be written and the direction of movement of the head. This includes 2 cases:

1. Initially, the Decoder starts off with in the state q_{copy} . While the state is still q_{copy} , the head writes the symbol at the i^{th} position in the encoder and moves right, until a blank symbol is seen. Once a blank symbol is reached, the tape rewrites the blank symbol, moves left and the state changes to q_{init} .
2. Once we move into q_{init} , the output is fully defined by the current state and symbol under the head.

To facilitate the first case, we make use of the cross attention layer, to get

$$\begin{aligned} Att(\mathbf{q}, \mathbf{K}^e, \mathbf{V}^e) &= [0, \dots, 0, \\ &\quad \mathbf{0}_q, \llbracket \alpha^{(i)} \rrbracket, 0, 0, 0, 0, \\ &\quad \beta^{(i)}, \mathbf{0}_s, 0, \\ &\quad 0, 0, 0, 0] \\ &= \mathbf{v}_{\beta^{(i)}}^e \end{aligned} \quad (21)$$

The details of this process are explained in lemma S.1(see sec. A.4) Adding in the residual connection, we have:

$$\begin{aligned} \mathbf{a}_i^1 = & \llbracket [q^{(i)}], [s^{(i)}], m^{(i-1)}, c^{(i)} \\ & \mathbf{0}_q, [\alpha^{(i)}], 0, 0, 0, 0, \\ & \beta^{(i)}, \mathbf{0}_s, 0, \\ & 1, i + 1, \frac{1}{(i + 1)}, \frac{1}{(i + 1)^2} \rrbracket \end{aligned} \quad (22)$$

Hereafter, we make use of the feed-forward layer to get:

$$\begin{aligned} O(\mathbf{a}_i^1) = & [-\llbracket [q^{(i)}], -\llbracket [s^{(i)}], -m^{(i-1)}, m^{(i)}, \\ & \llbracket [q^{(i+1)}], [\bar{v}^{(i)}], m^{(i)}, m^{(i-1)}, 0, 0, \\ & 0, \dots, 0 \\ & 0, \dots, 0 \rrbracket \end{aligned} \quad (23)$$

If the state is q_{init} then we set $[\bar{v}^{(i)}] = \mathbf{0}_s$, else we have $[\bar{v}^{(i)}] = [v^{(i)}]$. Note that this gives us $[\bar{v}^{(i)}] + [\alpha^{(i)}] = [v^{(i)}]$.

To get all the required values, we first project $\llbracket [q^{(i)}]$ and $\llbracket [s^{(i)}]$ to a one-hot encoding of $Q \times \Sigma$. from there, we can calculate all the required values in a look-up table fashion. if the state is q_{init} then we set $\llbracket [v^{(i)}] = \mathbf{0}_s$

The final output of this layer is then:

$$\begin{aligned} \mathbf{z}_i^1 = & [0, \dots, 0, c^{(i+1)} \\ & \llbracket [q^{(i+1)}], [v^{(i)}], m^{(i)}, m^{(i-1)}, 0, 0, \\ & \beta^{(i)}, \mathbf{0}_s, 0, \\ & 1, i + 1, \frac{1}{(i + 1)}, \frac{1}{(i + 1)^2} \rrbracket \end{aligned} \quad (24)$$

Decoder Layer 2: In this layer we calculate the symbol under the head in the next timestep. In order to do so, we first use the self attention layer to calculate $\llbracket [v^{(\ell(i+1))}]$ and $(\ell(i + 1))$ (For details, see sec A.7.):

$$\begin{aligned} Att(W_q^2 \mathbf{z}_i^2, W_k^2 \mathbf{Z}^2, W_v^2 \mathbf{Z}^2) = & [0, \dots, 0, \\ & 0, \dots, 0, \\ & 0, \llbracket [v^{(\ell(i+1))}] \rrbracket, (\ell(i + 1)), \\ & 0, 0, 0, 0] \end{aligned} \quad (25)$$

Adding the residual layer, we have

$$\begin{aligned} \mathbf{a}_i^2 = & [0, \dots, 0, c^{(i+1)} \\ & \llbracket [q^{(i+1)}], [v^{(i)}], m^{(i)}, m^{(i-1)}, 0, 0, \\ & \beta^{(i)}, \llbracket [v^{(\ell(i+1))}] \rrbracket, (\ell(i + 1)), \\ & 1, i + 1, \frac{1}{(i + 1)}, \frac{1}{(i + 1)^2} \rrbracket \end{aligned} \quad (26)$$

The feed-forward layer then gives $O_2(\mathbf{a}_i^2) = \llbracket [q^{(i+1)}], [v^{(\ell(i+1))}] - f_{perc}((\ell(i + 1) + 2 - (i + 1)), m^{(i-1)}, 0, -M, \dots - M) \rrbracket$ where M is a large negative value. The perceptron function in the \mathbf{s}_1 is added positionwise, and is 0 unless $\ell(i + 1) = i$. In this special case, it makes \mathbf{s}_1 contain only 0 or -1 which is converted into $\mathbf{0}_s$ by the ReLU activation in the output MLP. The same is also true for every field after the first 4, where we add a large negative value to make the ReLU output 0.

A.3 The Attention Mechanism

The attention mechanism in the Gaussian kernel is defined as follows:

$$Attn(\mathbf{Q}, \mathbf{K}, \mathbf{V}) = \mathbf{V}(\text{ColNorm}(\Phi(\mathbf{Q})^T \Phi(\mathbf{K}))) \quad (27)$$

where Φ is Φ_{RRS} (Eq 34) for Theorem 1 and Φ_{PRF} (Eq 33) for Theorem 2, and ω_i is sampled from a gaussian with zero mean and diagonal covariance. However, for the proof construction, we use a hard version of this attention mechanism, and limit ourselves to the standard gaussian for ω (since the mean and sigma is learnable, this can always be achieved). To begin with, we replace the kernels with their common dual, using lemma S.2 (sec A.6). In our construction, we do not require learnable means and variances, so we fix them to be 0_{d_q} and \mathbb{I} hereafter:

$$Attn(\mathbf{Q}, \mathbf{K}, \mathbf{V}) = \sum_{i=0}^{h-1} \mathbf{W}_O^i \mathbf{V} \left(\text{ColNorm} \left[\left[e^{-\frac{\|\mathbf{q}_l - \mathbf{k}_m\|^2}{2}} \right]_{l=0, m=0}^{d-1, d-1} \right] \right) \quad (28)$$

where $\llbracket f(l, m) \rrbracket_{l=0, m=0}^{\alpha, \beta}$ denotes an $\alpha \times \beta$ matrix whose $(l, m)^{th}$ entry is $f(l, m)$, $\text{ColNorm}(\mathbf{X})$ indicates the matrix \mathbf{X} with its columns normalised to and d is the dimension of the query/key vector.

While this definition does not seem to allow multiplying the exponent, one must remember that the query and key matrices are calculated using projection matrices, and any required scalar factor can be incorporated into them. Therefore, we define hard gaussian attention as:

$$\text{score}(\mathbf{u}, \mathbf{v}) = -\|\mathbf{u} - \mathbf{v}\|^2 \quad (29)$$

Hard attention is then computed as

$$Att(\mathbf{q}_i, \mathbf{K}, \mathbf{V}) = \frac{\sum_{j=0}^{n-1} \mathbb{I}[\text{score}(\mathbf{q}_i, \mathbf{k}_j) = (\max_{j'} \text{score}(\mathbf{q}_i, \mathbf{k}_{j'}))] \mathbf{v}_j}{\sum_{j=0}^{n-1} \mathbb{I}[\text{score}(\mathbf{q}_i, \mathbf{k}_j) = \max_{j'} (\text{score}(\mathbf{q}_i, \mathbf{k}_{j'}))] } \quad (30)$$

Here \mathbb{I} in the indicator function.

A.4 Lemma S.1

A.5 Statement

Given

$$\begin{aligned} \mathbf{q} &= [_, \dots, _, 1, i, _, _] \\ \mathbf{k}_j^e &= [0, \dots, 0, \\ &\quad 0, \dots, 0, \\ &\quad 0, \dots, 0, \\ &\quad j, -1, 0, 0] \\ \mathbf{v}_j^e &= [0, \dots, 0, \\ &\quad \mathbf{0}_q, \llbracket s^{(j)} \rrbracket, 0, 0, 0, 0, \\ &\quad j, \mathbf{0}_s, 0, \\ &\quad 0, 0, 0, 0] \end{aligned} \quad (31)$$

For $j \in \{0, \dots, n\}$, we need a construction that gives

$$\begin{aligned} Att(\mathbf{q}, \mathbf{K}^e, \mathbf{V}^e) &= [0, \dots, 0, \\ &\quad \mathbf{0}_q, \llbracket \alpha^{(i)} \rrbracket, 0, 0, 0, 0, \\ &\quad \beta^{(i)}, \mathbf{0}_s, 0, \\ &\quad 0, 0, 0, 0] \\ &= \mathbf{v}_{\beta^{(i)}}^e \end{aligned} \quad (32)$$

A.5.1 Proof

Note that while the key and value comes from the encoder, and is therefore fixed, the query comes from the decoder and thus can be projected as we please. It is easy to construct a projection matrix that gives $W_Q \mathbf{q} = [0, \dots, i, -1, 0, 0]$. Then we have $score(\mathbf{q}, \mathbf{k}_{j'}) = -\|i = j\|^2 = -(i - j)^2$, whose maxima on j' is unique and occurs at $i = \beta^{(j)}$. Thus, we have $Att(\mathbf{q}, \mathbf{K}^e, \mathbf{V}^e) = \mathbf{v}_{\beta^{(j)}}^e$, which is exactly what we wanted.

A.6 Lemma S.2

A.6.1 Statement

Let

$$\Phi_{PRF}(\mathbf{x}) = [\exp(-\|\mathbf{x}\| + \omega_0^T \mathbf{x}), \dots, \exp(-\|\mathbf{x}\| + \omega_{k-1}^T \mathbf{x})] \quad (33)$$

$$\Phi_{RKS}(\mathbf{x}) = \sqrt{\frac{2^m}{k}} [\cos(\omega_1^T x), \dots, \cos(\omega_k^T x), \sin(\omega_1^T x), \dots, \sin(\omega_k^T x)] \quad (34)$$

We want to show that if $\omega \sim \mathcal{N}(0, \mathbf{I})$ then the kernels as defined above corresponds to the *GMM kernel*, ie.

$$\Phi_{RKS}(\mathbf{X})\Phi_{RKS}(\mathbf{Y}) \approx \Phi_{PRF}(\mathbf{X})\Phi_{PRF}(\mathbf{Y}) \approx e^{-\frac{\|\mathbf{x}-\mathbf{y}\|^2}{2}} \quad (35)$$

A.6.2 Proof

Positive Random Features:The proof actually follows from a trivial extension of Lemma 1 in (Choromanski et al., 2021b), but we present it here end to end for the convenience of the reader.

First we observe that

$$\begin{aligned} e^{-\frac{\|\mathbf{x}-\mathbf{y}\|^2}{2}} &= e^{-\frac{\|\mathbf{x}\|^2 - 2\mathbf{x}^T \mathbf{y} + \|\mathbf{y}\|^2}{2}} \\ &= e^{-\frac{2*\|\mathbf{x}\|^2 - \|\mathbf{x}\|^2 - 2\mathbf{x}^T \mathbf{y} + 2*\|\mathbf{y}\|^2 - \|\mathbf{y}\|^2}{2}} \\ &= e^{-\|\mathbf{x}\|^2} e^{\frac{\|\mathbf{x}+\mathbf{y}\|^2}{2}} e^{-\|\mathbf{y}\|^2} \end{aligned} \quad (36)$$

Next we leverage the fact that $(2\pi)^{-d_q/2} \int e^{-\frac{\|\omega-\mathbf{c}\|^2}{2}} d\omega = 1$ in to evaluate the second factor above:

$$\begin{aligned} e^{\frac{\|\mathbf{x}+\mathbf{y}\|^2}{2}} &= (2\pi)^{-d_q/2} e^{\frac{\|\mathbf{x}+\mathbf{y}\|^2}{2}} \int e^{-\frac{\|\omega-\mathbf{x}+\mathbf{y}\|^2}{2}} d\omega \\ &= (2\pi)^{-d_q/2} \int e^{-\frac{\|\omega\|^2 + \|\mathbf{x}+\mathbf{y}\|^2 - \|\mathbf{x}+\mathbf{y}\|^2 - 2\omega^T \mathbf{x} - 2\omega^T \mathbf{y}}{2}} d\omega \\ &= (2\pi)^{-d_q/2} \int e^{-\frac{\|\omega\|^2}{2}} e^{\omega^T \mathbf{x}} e^{\omega^T \mathbf{y}} d\omega \\ &= \mathbb{E}_{\omega_i \sim \mathcal{N}(0, \mathbf{I})} (e^{\omega^T \mathbf{x}} e^{\omega^T \mathbf{y}}) \end{aligned} \quad (37)$$

The terms $e^{-\|\mathbf{x}\|^2}$ and $e^{-\|\mathbf{y}\|^2}$ in the last line of Eq.36 are independent of ω and can thus be pushed into the expectation. Finally, we approximate the expectation by sampling in order to get the required result.

Random Kitchen Sinks:For the second kernel, we start with Eq. 7.4.6 in Abramowitz & Stegun (1972) and extend it to vectors. We have,

$$\begin{aligned}
& \int_{\mathbb{R}^m} e^{-\|t\|^2} \cos(2\mathbf{t}^T \mathbf{x}) dt \\
&= \int_{\mathbb{R}^m} e^{-(t_0^2 + \sum_{i=1}^{m-1} t_i^2)} \cos\left(2x_0 t_0 + 2 \sum_{i=1}^{m-1} t_i x_i\right) dt_0 dt_1 \dots dt_{m-1} \\
&= \int_{\mathbb{R}^m} e^{-(t_0^2 + \sum_{i=1}^{m-1} t_i^2)} \cos(2x_0 t_0) \cos\left(2 \sum_{i=1}^{m-1} t_i x_i\right) dt_0 dt_1 \dots dt_{m-1} \\
&\quad - \int_{\mathbb{R}^m} e^{-(t_0^2 + \sum_{i=1}^{m-1} t_i^2)} \sin(2x_0 t_0) \sin\left(2 \sum_{i=1}^{m-1} t_i x_i\right) dt_0 dt_1 \dots dt_{m-1}
\end{aligned}$$

The second integral involving sin is odd and therefore evaluates to 0. That leaves us with:

$$\begin{aligned}
&= \int_{\mathbb{R}^m} e^{-(t_0^2 + \sum_{i=1}^{m-1} t_i^2)} \cos(2x_0 t_0) \cos\left(2 \sum_{i=1}^{m-1} t_i x_i\right) dt_0 dt_1 \dots dt_{m-1} \\
&= \int_{\mathbb{R}^{m-1}} \left(\int_{-\infty}^{\infty} e^{-t_0^2} \cos(2x_0 t_0) dt_0 \right) e^{-\sum_{i=1}^{m-1} t_i^2} \cos\left(2 \sum_{i=1}^{m-1} t_i x_i\right) dt_1 \dots dt_{m-1} \\
&= \frac{1}{2} \sqrt{\pi} e^{-x_0^2} \int_{\mathbb{R}^{m-1}} e^{-\sum_{i=1}^{m-1} t_i^2} \cos\left(2 \sum_{i=1}^{m-1} t_i x_i\right) dt_1 \dots dt_{m-1}
\end{aligned}$$

This process can now be repeated for every dimension of t and x to finally give:

$$\int_{\mathbb{R}^m} e^{-\|t\|^2} \cos(2\mathbf{t}^T \mathbf{x}) dt = \frac{\pi^{m/2}}{2^m} e^{-\|\mathbf{x}\|^2} \quad (38)$$

Using Eq. 38, we can now get

$$\begin{aligned}
\Phi_{RKS}(\mathbf{X})\Phi_{RKS}(\mathbf{Y}) &= \frac{2^m}{k} \sum_{i=0}^{k-1} (\cos(\omega_i^T \mathbf{x}) \cos(\omega_i^T \mathbf{y}) + \sin(\omega_i^T \mathbf{x}) \sin(\omega_i^T \mathbf{y})) \\
&= \frac{2^m}{k} \sum_{i=0}^{k-1} \cos(\omega_i(\mathbf{x} - \mathbf{y})) \\
&\approx 2^m \mathbb{E}_{\omega_i \sim \mathcal{N}(\mathbf{0}_m, \mathbb{I})} \cos(\omega(\mathbf{x} - \mathbf{y})) \\
&= 2^m \int_{\mathbb{R}^m} \frac{1}{(2\pi)^{m/2}} e^{-\frac{\|\omega\|^2}{2}} \cos\left(2\omega^T \frac{\mathbf{x} - \mathbf{y}}{2}\right) d\omega \\
&= \frac{2^m}{\pi^{m/2}} \int_{\mathbb{R}^m} e^{-\|\frac{\omega}{\sqrt{2}}\|^2} \cos\left(2\frac{\omega}{\sqrt{2}}^T \frac{\mathbf{x} - \mathbf{y}}{\sqrt{2}}\right) d\frac{\omega}{\sqrt{2}} \\
&= e^{-\frac{\|\mathbf{x} - \mathbf{y}\|^2}{2}}
\end{aligned} \quad (39)$$

In either case, the error stems from the approximation of the expectation by sampling, which can be made arbitrarily small by increasing k

A.7 Lemma S.3

A.7.1 Statement

Given,

$$\begin{aligned} \mathbf{z}_i^1 = & [0, \dots, 0, c^{(i+1)}, \\ & \llbracket q^{(i+1)} \rrbracket, \llbracket v^{(i)} \rrbracket, m^{(i)}, m^{(i-1)}, 0, 0, \\ & \beta^{(i+1)}, \mathbf{0}_s, 0, \\ & 1, (i+1), \frac{1}{(i+1)}, \frac{1}{(i+1)^2}] \end{aligned} \quad (40)$$

we need a construction that gives

$$\begin{aligned} Att(W_q^2 \mathbf{z}_i^2, W_k^2 \mathbf{z}_i^2, W_v^2 \mathbf{z}_i^2) = & [0, \dots, 0, \\ & 0, \dots, 0, \\ & 0, \llbracket v^{(\ell(i+1))} \rrbracket, (\ell(i+1)), \\ & 0, 0, 0, 0] \end{aligned} \quad (41)$$

A.7.2 Proof

We set the weight matrices to get $\mathbf{q}_j = W_q^2 \mathbf{z}_j^2 = [0, \dots, 0, c^{(j+1)}, 0, 0]$, $\mathbf{k}_j = W_k^2 \mathbf{z}_j^2 = [0, \dots, 0, c^{(j)} = c^{(j+1)} - m^{(i)}, 0, \frac{1}{(j+1)}]$ and $\mathbf{v}_j = W_v^2 \mathbf{z}_j^2 = [0, \dots, 0, \llbracket v^{(j)} \rrbracket, j, 0, 0, 0, 0]$. All these are partial permutations and therefore can be done using appropriate binary matrices.

Note that the required output is exactly the value at $j = \ell(i+1)$, so it is sufficient to show that the $score(\mathbf{q}_i, \mathbf{k}_j)$ is maximised in j for $j = \ell(i+1)$, i.e.

$$j = \begin{cases} \max\{j' | c^{(j')} = c^{(i+1)}\}, & \text{if } \exists j' \text{ s.t. } c^{(j')} = c^{(i+1)} \\ i, & \text{otherwise} \end{cases} \quad (42)$$

Now we have $score(\mathbf{q}_i, \mathbf{k}_j) = -(c^{(i+1)} - c^{(j)})^2 - \frac{1}{(j+1)^2}$. For all j such that $c^{(i+1)} \neq c^{(j)}$, the $score$ is almost -1 since c is an integer. If there $\exists j' \text{ s.t. } c^{(j')} = c^{(i+1)}$ then the corresponding $score$ is greater than -1 , and the maxima is achieved at the highest such value of j . If such j does not exist however, then $\forall j < i$, $score(\mathbf{q}_i, \mathbf{k}_j) < -1 - \frac{1}{(i+1)^2}$ and therefore, the maxima is achieved at $j = i$.

B Mean Square Error of Linear Approximations

In this section, we calculate the Variance/Mean Square Error(MSE) in the Linear approximation of the Gaussian Kernel. Our proof is based on the similar proof in Choromanski et al. (2021b).

B.1 Random Kitchen Sinks

B.1.1 Statement

For a GMM-RKS estimator with m samples for a Normal distribution with mean vector μ and Covariance Matrix $\Sigma = S^T S$, the variance of the estimate around its mean is given by:

$$MSE(\phi_{\text{GMM-RKS}}(q)^T \phi_{\text{GMM-RKS}}(k)) = \frac{2}{m} \cos^2(\mu^T(k - q))(1 - \exp(-\|S^T(k - q)\|^2))^2 \quad (43)$$

B.1.2 Proof

$$\begin{aligned}
& MSE(\phi_{\text{GMM-RKS}}(q)^T \phi_{\text{GMM-RKS}}(k)) \\
&= \frac{1}{m^2} Var_{\omega_i \sim \mathcal{N}(\mu, \Sigma), \chi_i \sim \mathcal{N}(-\mu, \Sigma)} \left(\sum_{i=1}^m (\cos(\omega_i^T q) \cos(\omega_i^T k) + \sin(\omega_i^T q) \sin(\omega_i^T k)) \right. \\
&\quad \left. + \cos(\chi_i^T q) \cos(\chi_i^T k) + \sin(\chi_i^T q) \sin(\chi_i^T k) \right) \\
&= \frac{1}{m^2} Var_{\omega_i \sim \mathcal{N}(\mu, \Sigma), \chi_i \sim \mathcal{N}(-\mu, \Sigma)} \left(\sum_{i=1}^m (\cos(\omega_i^T (q - k)) + \cos(\chi_i^T (q - k))) \right) \\
&= \frac{1}{m^2} Var_{\eta_i \sim \mathcal{N}(0, \mathbb{I})} \left(\sum_{i=1}^m (\cos((\eta_i^T S^T + \mu^T)(q - k)) + \cos((\eta_i^T S^T - \mu^T)(q - k))) \right) \tag{44} \\
&= \frac{4}{m^2} Var_{\eta_i \sim \mathcal{N}(0, \mathbb{I})} \left(\sum_{i=1}^m \cos(\eta_i^T S^T (q - k)) \cos(\mu^T (q - k)) \right) \\
&= \frac{4}{m^2} \cos^2(\mu^T (q - k)) Var_{\eta_i \sim \mathcal{N}(0, \mathbb{I})} \left(\sum_{i=1}^m \cos(\eta_i^T S^T (q - k)) \right) \\
&= \frac{4}{m} \cos^2(\mu^T (q - k)) Var_{\eta \sim \mathcal{N}(0, \mathbb{I})} \cos(\eta^T (S^T (q - k))) \\
&= \frac{2}{m} \cos^2(\mu^T (q - k)) (1 - \exp(-\|S^T (q - k)\|^2))^2
\end{aligned}$$

Note that there is a slight abuse of notation in that ω and χ are not independently sampled, but are transforms of the same sample, making the change of variable valid. Since all η are iid, we can pull the summation out of the variance. Thereafter we apply Lemma 1 from Yu et al. (2016a) to calculate the final variance.

B.2 Positive Random Features

For a GMM-PRF estimator with m samples for a Normal distribution with mean vector μ and Covariance Matrix $\Sigma = S^T S$, the variance of the estimate around its mean is given by:

$$\begin{aligned}
& MSE(\phi_{\text{GMM-PRF}}(q)^T \phi_{\text{GMM-PRF}}(k)) \\
&= \frac{1}{m} \exp(-2(\|q\|^2 + \|k\|^2 - \mu^T (q + k))) (\exp(2\|S^T (q + k)\|) - \exp(\|S^T (q + k)\|)) \tag{45}
\end{aligned}$$

B.2.1 Proof

$$\begin{aligned}
& MSE(\phi_{\text{GMM-PRF}}(q)^T \phi_{\text{GMM-PRF}}(k)) \\
&= \frac{1}{m^2} Var_{\omega_i \sim \mathcal{N}(\mu, \Sigma)} \left(\sum_{i=1}^m (\exp(\omega_i^T (q + k)) - \|q\|^2 - \|k\|^2) \right) \\
&= \frac{1}{m} \exp(-2(\|q\|^2 + \|k\|^2)) Var_{\omega \sim \mathcal{N}(\mu, \Sigma)} \exp(\omega^T (q + k)) \\
&= \frac{1}{m} \exp(-2(\|q\|^2 + \|k\|^2)) Var_{\eta \sim \mathcal{N}(0, \mathbb{I})} (\exp(\eta^T S^T (q + k) + \mu^T (q + k))) \tag{46} \\
&= \frac{1}{m} \exp(-2(\|q\|^2 + \|k\|^2 - \mu^T (q + k))) \\
&\quad (\mathbb{E}_{\eta \sim \mathcal{N}(0, \mathbb{I})} (\exp(2\eta^T S^T (q + k))) - (\mathbb{E}_{\eta \sim \mathcal{N}(0, \mathbb{I})}^2 (\exp(\eta^T S^T (q + k)))) \\
&= \frac{1}{m} \exp(-2(\|q\|^2 + \|k\|^2 - \mu^T (q + k))) (\exp(2\|S^T (q + k)\|) - \exp(\|S^T (q + k)\|))
\end{aligned}$$

Where the last step follows from Eq. 16 in Choromanski et al. (2021b) which in turn follows from the fact that GMM-PRF is an unbiased estimator for gaussians.

Model	<i>Image</i>
Random Predictor	10.00
Baseline Models	
Softmax Trans.(Vaswani et al.)	42.44
Synthesizer(Tay et al.)	41.61
Sinkhorn(Tay et al.)	41.23
Sparse Trans.(Child et al.)	44.24
Reformer(Kitaev et al.)	38.07
Local Attention (Parmar et al.)	41.46
Longformer(Beltagy et al.)	42.22
Linformer(Wang et al.)	38.56
Big Bird(Zaheer et al.)	40.83
LinearElu(Katharopoulos et al.)	42.34
Performer(Choromanski et al.)	<u>42.77</u>
Kernelized Transformers	
GMM-RKS (Eq. 5)	42.33
FASTFOOD-RKS (Eq. 6)	36.74
GENERATIVE-RKS (Eq. 8)	39.84
GMM-PRF (Eqs. 9, 10)	39.94
FASTFOOD-PRF (Eqs. 9, 12)	38.31
GENERATIVE-PRF (Eqs. 9, 11)	40.01

Table 5: Experimental results on the *Image* dataset with 1024 tokens from *LRA* benchmark.

C Experimental Details

C.1 Source Code

We implemented KL-TRANSFORMERS in Python 3 and PyTorch (Paszke et al., 2019) and plan to open-source the code for reproducing all experiments upon acceptance.

C.2 LRA image dataset results

For completeness we also give results on *Image* datasets from LRA task where a $N \times N$ image is flattened into a sequence of N^2 pixels which is then provided as input to the model. The gray-scaled CIFAR10 image classification dataset (Krizhevsky, 2009) is used, resulting in a sequence length of 1024.

C.3 Hyperparameters for LRA Tasks

Further Notes:

- To benchmark memory in Figure 3, we used a batch size of 32 for *Text* and a batch size of 2 for *Retrieval*.
- For GMM-RKS and GMM-PRF the number of components C in the mixture was set to $C = 2$.

Parameter	ListOps	Text	Retrieval	Image
Batch Size	32	32	32	256
Learning Rate	5×10^{-3}	5×10^{-2}	5×10^{-2}	5×10^{-4}
Training Steps/Epochs	10K/NA	20K/NA	5K/NA	NA/200
Optimizer	Adam with Weight Decay ($\beta_1 = 0.9, \beta_2 = 0.98$)			
Weight Decay	0.1	0.1	0.1	0.0
Warmup Steps	1000	8000	8000	175
Scheduler	Sqrt Decay	Sqrt Decay	Sqrt Decay	Cosine Decay
Loss	Cross Entropy			
Sequence Length	2000	4000	4000	1024
Num. Layers	6	4	4	1
Num. Heads	8	4	4	8
Embedding Dim.	512	256	128	128
Key/Query/Value Dim.	64	64	32	8
Feedforward Dim.	2048	1024	512	128
Dropout Rate	0.1	0.1	0.1	0.3
Activation Function	Gelu	Gelu	Gelu	Gelu
Positional Encoding	Sinusoidal	Sinusoidal	Sinusoidal	Learnable
Pooling Mode	CLS	CLS	CLS	CLS

Table 6: Hyperparameters for *LRA* tasks.

Model	ListOps	Text	Retrieval	Image
GMM-RKS	256	128	64	128
FASTFOOD-RKS	64	64	32	8
GENERATIVE-RKS	256	256	128	128
GMM-PRF	256	256	128	128
FASTFOOD-PRF	64	64	32	8
GENERATIVE-PRF	128	128	64	8

Table 7: Number of random samples M used within each KL-TRANSFORMER.

C.4 Hyperparameters for GLUE Tasks

Parameter	Value(s)
Pre-Training Batch Size	64
Batch Size	64
Pre-Training Learning Rate (η_{pre})	5×10^{-4}
Pre-Training Learning Rate at Step i	$\min(\frac{i}{10000}, \frac{I_{\text{pre}}-i}{I_{\text{pre}}-10000}) * \eta_{\text{pre}}$
Training Learning Rate (η_{train})	$\{2 \times 10^{-3}, 1 \times 10^{-4}, 5 \times 10^{-4}, 2 \times 10^{-5}, 5 \times 10^{-6}\}$
Training Learning Rate at Step i (η_{train})	$\min(\frac{10i}{I_{\text{tune}}}, \frac{I_{\text{tune}}-i}{0.9 * I_{\text{tune}}}) * \eta_{\text{train}}$
Pre-Training Epochs	5
Training Epochs	10
Optimizer	Adam with Weight Decay ($\beta_1 = 0.9, \beta_2 = 0.999$)
Weight Decay	0.01
Loss	Cross Entropy
Sequence Length	512
Num. Layers	3
Num. Heads	10
Embedding Dimension	300
Key/Query/Value Dimension	64
Transformer Feedforward Dimension	512
Classifier Feedforward Dimension	128
Dropout Rate	0.1
Transformer Activation Function	Gelu
Classifier Activation Function	Tanh
Positional Encoding	Sinusoidal
Pooling Mode	CLS
Num. of Samples from Distribution	{64, 128}

Table 8: Hyperparameters for *GLUE* tasks. Where multiple parameters were tried, they are listed in curly brackets. I_{pre} denotes the total number of pre-training steps, whereas I_{tune} denotes the total number of fine-tuning steps on each *GLUE* task.

Our model has significantly fewer number of parameters as compared to Devlin et al. (2019) and therefore we perform poorer on than them on all datasets. They use 24 layers with 16 heads each. If reported in the same order as the columns of Table 3, their numbers would look like: 97.5, 89.3/85.4, 72.1/89.3, 87.2/86.4, 92.7, 65.1, 70.1.

While we had to limit model sizes due to resource limitations, this handicaps all models equally, and therefore should not prevent comparison across various models reported in our paper.

C.5 Further Results on Efficiency Benchmarks

Figure 7 shows how much memory each model uses. Figure 8 plots this memory usage against the model performance

C.6 Correlation of Variance Metrics

Figures 9 and 10 show the correlation of Average Gain by Voting with the other twp variance metrics for the text and retrieval tasks respectively

Layer	Head	Minimum	Maximum	Mean
1	1	7.601e-7	4.584e-1	3.531e-2
	2	2.380e-8	4.863e-1	3.576e-2
	3	1.400e-5	4.469e-1	3.319e-2
	4	4.214e-6	4.197e-1	3.208e-2
2	1	4.242e-6	2.790e-1	3.070e-2
	2	2.971e-6	3.238e-1	3.161e-2
	3	5.081e-6	2.842e-1	3.078e-2
	4	5.212e-7	3.006e-1	3.086e-2
3	1	2.297e-6	2.219e-1	2.872e-2
	2	7.094e-6	2.036e-1	2.594e-2
	3	1.074e-7	1.953e-1	2.772e-2
	4	6.330e-9	1.836e-1	2.442e-2

Table 9: Distribution of Eigenvalues of covariances of GMM-RKS model for the *Text* task

Layer	Head	Minimum	Maximum	Mean
1	1	1.363e-5	9.660e-2	2.440e-2
	2	6.659e-5	7.900e-2	2.200e-2
	3	7.241e-6	9.050e-2	2.810e-2
	4	2.760e-5	7.790e-2	2.630e-2
2	1	2.068e-5	7.520e-2	2.430e-2
	2	2.386e-5	7.580e-2	2.400e-2
	3	7.256e-6	7.400e-2	2.370e-2
	4	1.911e-4	8.080e-2	2.680e-2
3	1	2.871e-5	6.710e-2	2.570e-2
	2	6.117e-6	7.370e-2	2.190e-2
	3	7.830e-6	6.600e-2	2.010e-2
	4	2.186e-5	7.620e-2	2.810e-2

Table 10: Distribution of Eigenvalues of covariances of GMM-PRF model for the *Text* task

Layer	Head	Minimum	Maximum	Mean
1	1	4.011e-05	4.994e-01	5.998e-02
	2	4.250e-05	2.294e-01	5.390e-02
	3	1.918e-04	3.427e-01	5.842e-02
	4	5.615e-06	3.943e-01	5.866e-02
2	1	3.232e-06	2.605e-01	5.469e-02
	2	2.746e-06	2.581e-01	5.333e-02
	3	6.364e-06	2.329e-01	5.091e-02
	4	2.071e-05	1.743e-01	5.020e-02
3	1	4.358e-05	1.919e-01	5.157e-02
	2	1.143e-04	1.738e-01	4.819e-02
	3	2.546e-05	1.735e-01	4.705e-02
	4	9.697e-07	2.075e-01	4.982e-02

Table 11: Distribution of Eigenvalues of covariances of GMM-RKS model for the *Retrieval* task

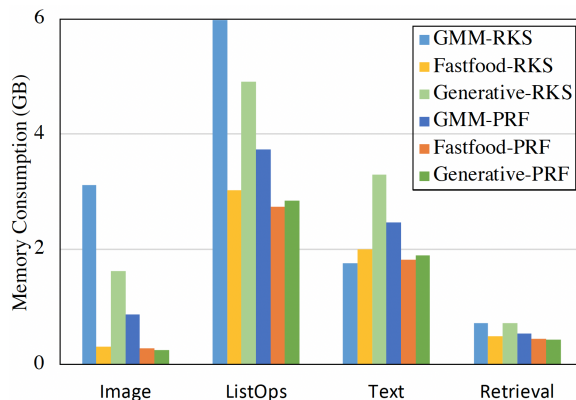


Figure 7: Peak memory used by KL-TRANSFORMERS across different datasets.

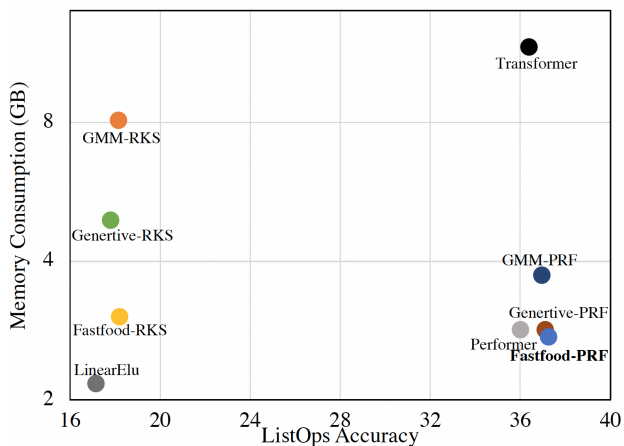


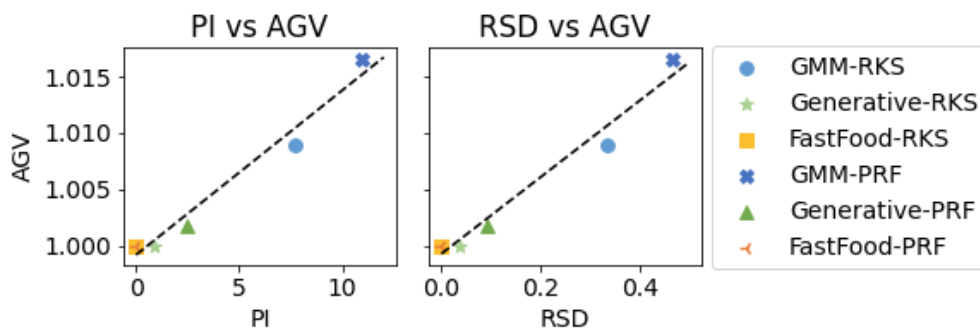
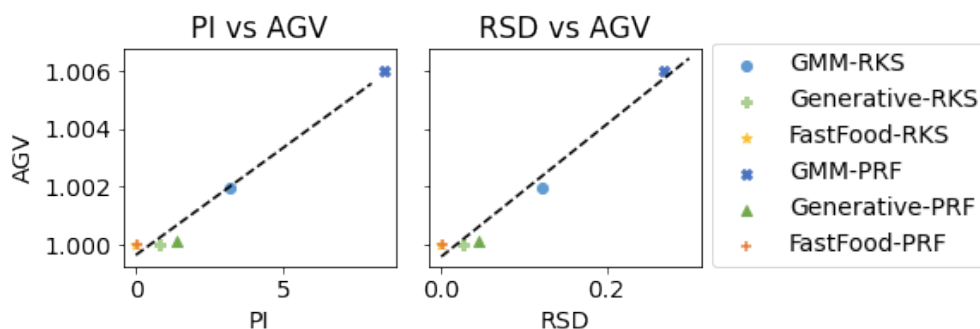
Figure 8: We demonstrate the peak memory consumption (y-axis) and performance (x-axis) of the various Kernelized Transformer architectures on the ListOps dataset from LRA. Memory usage refers to per device memory usage across each GPU.

C.7 Eigenvalues of Trained Models

D Ablation Studies

D.1 FastFood Attention

In the main paper, we use FastFood-SGB, which has all the diagonal matrices learnable. However, B and G matrices have a very special structure (their elements being drawn from $Bernoulli_{\{-1,1\}}(0.5)$ and $\mathcal{N}(0, 1)$ respectively), which is lost if we make them learnable. Therefore, it makes sense to have *FastFood-S*, which only has S learnable. Finally, we can also have everything fixed, giving us the basic *FastFood* version. The results of these two versions, along with the original FastFood-SGB kernel on the *GLUE* benchmark are summarised in Table 13. As one can see, FastFood-SGB is either the best or close to it except for WNLI and CoLA, therefore we choose to use this version for our main analysis.

Figure 9: Correlation between AGV and the other two variance metrics on the **Text** task.Figure 10: Correlation between AGV and the other two variance metrics on the **Retrieval** task.

E Sparsity Synthetic Experiment

E.1 Task Description

Given a sequence of ordered pairs (v_i, a_i) , where $v_i \in \{-1, 1\}$ and $a_i \in \{0, 1\}$, the task is to output $\sum_{i=0}^L v_i a_i$. Here, v_i can be seen as the value of a given position, while a_i indicates whether or not we need to attend to that position. The dataset is generated by (pseudo-randomly flipping a coin independently for a_i and v_i). The bias in the flip for a_i defines the sparsity of the dataset. The flip for v_i is appropriately biased to ensure that no prefix has an absolute sum of more than 4. The final prediction is outputted as a 9-way classification over integer values between -4 and 4 (both

Layer	Head	Minimum	Maximum	Mean
1	1	8.225e-05	2.114e-01	4.818e-02
	2	5.386e-05	1.525e-01	4.066e-02
	3	9.659e-05	1.707e-01	5.638e-02
	4	1.498e-07	1.467e-01	4.166e-02
2	1	1.294e-06	9.798e-02	3.024e-02
	2	9.306e-05	1.289e-01	4.334e-02
	3	4.300e-06	1.865e-01	4.846e-02
	4	2.418e-05	1.047e-01	4.458e-02
3	1	2.466e-08	1.133e-01	3.987e-02
	2	2.291e-04	1.429e-01	5.099e-02
	3	3.997e-05	1.134e-01	3.380e-02
	4	6.653e-05	1.129e-01	2.827e-02

Table 12: Distribution of Eigenvalues of covariances of GMM-PRF model for the *Retrieval* task

Dataset	SST2 (acc)	MRPC (acc)	MRPC (f1)	QQP (acc)	QQP (f1)	MNLI (mat)	MNLI (mis)	QNLI (acc)	WNLI (acc)	RTE (acc)	CoLA (MCorr)
FastFood	0.814	0.713	0.820	0.811	0.738	0.571	0.568	0.629	0.634	0.563	0.152
FastFood-S	0.807	0.706	0.822	0.810	0.741	0.571	0.571	0.642	0.606	0.570	0.101
FastFood SGB	0.828	0.707	0.820	0.810	0.739	0.569	0.572	0.638	0.592	0.563	0.129

Table 13: Ablation studies using FastFood variants on the *GLUE* benchmark.

Dataset Sparsity	Checkpoint Acc.(%)	GMM-RKS		GMM-PRF		GMM-RKS/GMM-PRF	
		Std. Dev.	Abs. Mean	Std. Dev.	Abs. Mean	Std. Dev.	Abs. Mean
0.1	20	0.083064	0.144132	0.079822	0.139948	0.960974	0.97097
	40	0.094528	0.16609	0.11077	0.193444	1.171828	1.164689
	60	0.099791	0.176456	0.116044	0.201462	1.162868	1.141712
	80	0.131252	0.228456	0.154802	0.275594	1.179433	1.206332
0.5	20	0.069646	0.121306	0.434024	0.53019	6.231835	4.370671
	40	0.11552	0.201468	6.432806	12.17245	55.68558	60.41891
	60	0.142631	0.249917	3.752173	5.886064	26.30681	23.55206
	80	0.166899	0.295308	22.46943	42.14157	134.6289	142.7036
0.9	20	0.059153	0.102415	0.065438	0.115866	1.106237	1.131343
	40	0.108255	0.186704	0.123171	0.211465	1.137784	1.132622
	60	0.119243	0.206855	0.126247	0.217067	1.058737	1.049365
	80	0.136816	0.240525	0.168633	0.295976	1.232546	1.230542

Table 14: Means and Variances of gradients received at the classifier layer for the synthetic experiment

inclusive). The bias against higher absolute values causes -4 and 4 classes to appear less often. This is balanced out by overgeneration and sampling.

We generate 3 datasets corresponding to sparsities 0.1, 0.5 and 0.9. Each dataset has $200K$ instances, of sequence length 200. Of these, we use 80% as the training set and the rest for validation.

E.2 Model Description

We use a 3 layer transformer with $d_{model} = d_{feedforward} = 64$ and $d_{query} = d_{value} = 16$. The input is encoded as a 3-d many-hot vector ($v_i = 1, v_i = -1, a_i$). this is then passed through an embedding layer and added to learnable position embeddings and passed through the transformer. The final embedding of the 0^{th} position is then passed through a hidden layer with 64 units and then passed on to the final layer for a 9-way softmax. For both linear attention models, we use 64 samples.

All models are trained using AdamW optimizer with $\beta_2 = 0.98$, $\epsilon = 10^{-9}$, weight decay=0.1, Learning Rate= 5×10^{-6} and all other parameters set to default. We use SGD with a batch size of 400 and cross entropy loss.

E.3 Gradients

We create checkpoints for the GMM-RKS and GMM-PRF models when they first achieve validation accuracies of 20%, 40%, 60% and 80%. For each of these checkpoints, we pass the first 50 validation datapoints and record the gradients on the classifier layer. This process is repeated 50 times. Thereafter, we calculate the mean and standard deviation of gradients to each neuron. To avoid cancellation of opposite signs, the mean is calculated over absolute values. The final reported numbers are averages over the 64 neurons. The results are shown in Table 14